

Quantum approaches to music cognition

Peter beim Graben^{a,*}, Reinhard Blutner^b

^a*Brandenburgische Technische Universität Cottbus – Senftenberg,
Institute of Electronics and Information Technology,
Department of Communications Engineering,
Cottbus, Germany*

^b*Emeritus Universiteit van Amsterdam,
ILLC,
Amsterdam, Netherlands*

Abstract

Quantum cognition emerged as an important discipline of mathematical psychology during the last two decades. Using abstract analogies between mental phenomena and the formal framework of physical quantum theory, quantum cognition demonstrated its ability to resolve several puzzles from cognitive psychology. Until now, quantum cognition essentially exploited ideas from projective (Hilbert space) geometry, such as quantum probability or quantum similarity. However, many powerful tools provided by physical quantum theory, such as symmetry groups and their representation theories, particularly local gauge symmetries and their connection to physical forces, have not been utilized in the field of quantum cognition research so far. This is somewhat astonishing as “mental forces” or “mental energies” appear as important metaphorical concepts in cognitive science. One particular example is music psychology, where static or dynamic tonal attraction phenomena are computationally often modeled in terms of metaphorical forces. Inspired by seminal work by Guerino Mazzola on the connection between musical forces and symmetries in tonal music, our study aims at elucidating and reconciling musical forces in the framework of quantum cognition. Based on the funda-

*Corresponding author

Email address: peter.beimgraben@b-tu.de (Peter beim Graben)

mental transposition symmetry of tonal music, as reflected by the circle of fifths, we develop different wave function descriptions over this underlying tonal space, governed by a Schrödinger equation containing different interaction energies. We present quantum models for static and dynamic tonal attraction and compare them with traditional computational models in musicology. Our approach replicates and also improves predictions based on symbolic models of music perception.

Keywords: music psychology, tonal attraction, quantum cognition, tonal space, harmonic analysis

Highlights.

- Quantum models for tonal attraction are compared with symbolic models in musicology
- Symbolic models of music cognition are parsimoniously rendered from our approach
- Tones appear as Gestalts, i.e. wave fields over the circle of fifths
- A connection between musical forces and symmetries in tonal music is established
- Discrete tonal scales emerge from fundamental musical transposition symmetry

1. Introduction

When the founding fathers of modern quantum physics, such as Niels Bohr (1950) or Wolfgang Pauli (1950), speculated about the tentative relevance of their theoretical developments for other areas of science, such as biology, psychology, sociology, or philosophy (cf. beim Graben and Atmanspacher (2009) for discussion), they could hardly imagine that *quantum cognition* has nowadays become an important discipline of mathematical psychology with applications in economics (Khrennikov 2010), decision theory (Busemeyer and Bruza

2012), categorization (Aerts 2009), language (Blutner 2012, beim Graben 2014), and even music (Chiara et al. 2015, Blutner 2015, beim Graben and Blutner 2017).

Until now, quantum cognition applies the mathematical techniques of Hilbert space geometry, projective lattices, noncommutative operator algebras, tensor product representations, and the resulting calculus of quantum probabilities (von Neumann 1955) as phenomenological instruments for modeling cognitive states and processes that seemingly resisted traditional computational modeling, e.g. in terms of classical probability theory, Bayesian inferences, or Markov chains. In this way, quantum models have been successfully applied to several paradoxical findings from cognitive psychology (Pothos and Busemeyer 2013, Busemeyer and Bruza 2012).

However, this *does not* mean that the brain, or particular neural networks have to be considered as quantum computers, i.e. as physical machines whose computation is necessarily described through quantum mechanics at the molecular or atomic level (Pothos and Busemeyer 2013). Instead, the phenomenological success of quantum cognition approaches to psychological puzzles has recently been explained by Blutner and beim Graben (2013, 2016) and by Lambert-Mogiliansky and Dubois (2016) on perspectival restrictions of the limited human mind. In particular, Blutner and beim Graben (2016) have shown that complementary heuristic perspectives lead to Hilbert space projector lattices in a given representation.

The study of Blutner and beim Graben (2016) was, to our knowledge, the first application of algebraic representation theory to quantum cognition. However, the mathematical apparatus of quantum theory, as employed in theoretical physics, presents a much broader array of formal tools, such as wave functions and quantum fields, symmetries and symmetry breaking, local gauge invariance and forces, frustrated connections and unitarily non-equivalent representations (Haag 1992) that could be promising for applications in the cognitive domain as well.

Of particular interest is Gestalt psychology (Köhler 1969) where sensational fields and their symmetries have been related to the wholeness of physical fields. Köhler (1969) illustrates visual Gestalt effects by means of the famous Fraser illusion (Fraser 1908), reproduced in Fig. 1(a). Here, several

concentric circles of twisted cords appear as deformed “round squares” due to the interaction with the checkerboard background. We suggest here that the background patterns generate virtual forces causing the deformation of the circles in Fig. 1(a). These forces may be regarded as a “visual gauge field”.

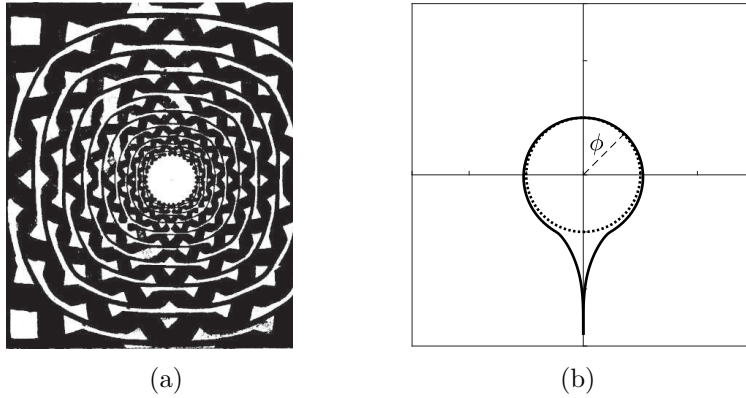


Figure 1: Circle deformations. (a) Fraser illusion [Fraser (1908, Fig. 8)] illustrating the square deformation of twisted-cord circles in a checkerboard background. The background may be regarded as visual gauge field. (b) Deformation of the unit circle (dotted) according to the quantum model presented below (solid). The phase angle ϕ denotes musical interval.

As another example, Köhler (1969) explains musical melodies and chords as acoustic Gestalts as they exhibit transposition symmetry (Balzano 1980, Mazzola 1990, 2002, Mannone and Mazzola 2015), which means that musical patterns remain invariant under translations along the important circle of fifths (however, see Bod (2002) for a controversial viewpoint). We illustrate the circle of fifths as the dotted unit circle in Fig. 1(b) also indicating a transposition angle ϕ for a musical interval. It is the aim of the present study to apply concepts from physical quantum theory that have originally been developed in analogy to classical field theory (Schrödinger 1926) to the domain of tonal attraction in the psychology of music, thereby extending and elaborating our previous work on quantum approaches to music cognition (Blutner 2015, beim Graben and Blutner 2017). One special result of our study is the deformation of the circle of fifths according to the solid line shown in Fig. 1(b). Also this construction rests on an important physical symmetry, the invariance of the line element in Einstein’s general theory of relativity.

The term “tonal attraction” refers to the idea that melodic or voice-leading pitches tend toward other pitches in greater or lesser degrees, and has been empirically investigated by means of *probe tone experiments* (Krumhansl and Shepard 1979, Krumhansl 1979), which can be regarded as priming experiments in music psychology: In each trial, a subject is presented with a priming context (e.g. a scale, a chord, or a cadence) that establishes a tonal key, say, C major, which is followed by a probe tone randomly chosen from the twelve tones of the chromatic scale (see Sect. 2.1 for details). Subjects are then asked to rate the amount of attraction exerted by the priming context upon the probe tone. Depending on the instruction, one can distinguish between probe tone experiments on static or dynamic attraction (Parncutt 2011). In the static attraction paradigm subjects are asked to rate *how well the probe tone fits into* the preceding context (Krumhansl and Kessler 1982), while in the dynamic attraction paradigm subjects are asked to rate *how well the probe tone completes or resolves* the preceding context (Temperley 2008, Woolhouse 2009). The difference between these different instructions is illustrated as follows: In the static attraction experiment a C major context primes the C major key such that C as a probe tone receives maximal attraction, followed by the members of the tonic triad G and E. By contrast, in the dynamic attraction experiment a C major context primes the F major key because the triad CEG is the dominant of F major which is resolved by its tonic triad FAC, making the probe tone F most likely, followed by C and then A (Woolhouse 2009).

There are essentially two research lines for computational models of tonal attraction data. The first, psychoacoustic bottom-up models are inspired by Hermann von Helmholtz’ (1877) attempts on spectral representations (Milne et al. 2011, 2015, Stolzenburg 2015). The second, cognitive top-down models go back to Lerdahl and Jackendoff’s (1983) generative theory of tonal music, using either hierarchically structured representations of tonal space (Lerdahl 1988, 1996, Krumhansl and Kessler 1982, Krumhansl and Cuddy 2010) or statistical correlations in large music corpora that are modeled by probabilistic approaches, such as Gaussian Markov chains (Temperley 2007, 2008). The former bottom-up models involve “smearing” or coarse-graining of spectral features. The latter top-down models, on which we put the focus in our study, often refer to metaphorical notions of musical forces.

The application of physical metaphors is quite common in theories of

music. The basic assumption seems to be that our experience of musical motion is in terms of our experience of physical motion and their underlying forces. For example, Schönberg speaks about musical forces when he explains the resolution of chords in cadences where the tonic attracts the dominant (Schönberg 1978, p. 58). In addition, Larson and van Handel (2005) and, more recently, Larson (2012) proposed three musical forces that generate melodic completions. These forces are called *gravity*, *inertia*, and *magnetism*, respectively:

Musical gravity is the tendency (attributed by a listener) of a note (heard as ‘above a stable platform’) to descend (to that platform) [...]. Musical magnetism is the tendency (attributed by a listener) of an unstable note to move to the closest stable pitch, a tendency that grows stronger as we get closer to that goal. [...] Musical inertia is the tendency (attributed by a listener) of a pattern of motion to continue in the same fashion, where the meaning of ‘same’ depends on how that pattern is represented in musical memory. (Larson and van Handel 2005)

These forces should be regarded as conceptual metaphors in the sense of Lakoff and Johnson (1980). They structure our musical cognition in analogy with falling, inert and attracting physical bodies. Physical forces are represented in our naive common sense physics or folk physics. Analogously, musical forces cause musical dynamics in the naive sense, that the impact of gravity yields to either ascending or descending melodic lines, depending on the position of a gravitation center. Magnetism should be as larger as closer a currently played tone is to a neighboring force center. And inertia refers to the observation that an already ascending or descending melody will remain ascending or descending in the sequel.

It goes without noting that naive physics (folk physics) and modern physics are completely different systems. Folk physics describes the perception of physical motion and physical forces by untrained human. In modern physics, however, forces are closely related to symmetry and symmetry breaking. According to a famous theorem of Emmy Noether, any (continuous) symmetry is accompanied with a conservation law. Conservation of momentum (i.e. the product of a particle’s mass with its velocity), e.g., as

expressed by Newton’s first law, is related to the homogeneity of space: if it is not possible to highlight a distinguished point in space, then momentum does not change in the course of time. By contrast, the presence of a force center as a distinguished point breaks the homogeneity of space and momentum evolves according to Newton’s third dynamical law: the particle is either attracted or repelled by the force center, resulting in positive or negative acceleration, respectively.

However, although forces are related to symmetry breaking, they obey a much deeper kind of symmetry, called local gauge symmetry in quantum field theory. There, matter is described by a wave function (governed by a Schrödinger or Dirac equation) and forces result from the coupling of the wave function with interaction fields. Locally gauging these interactions by the calibration of measurement devices is compensated by an unobservable phase shift of the matter’s wave function. Therefore, it is always possible to make forces locally vanishing by means of a local gauge transformation. A nice example for such a gauge symmetry is provided by Einstein’s general relativity theory where gravity vanishes in a free-falling reference system which is described by rulers and clocks whose calibration depends on space and time. These gauges change the local representation of space and time in certain coordinate systems. However, the spatiotemporal distance of events, expressed by the line element may not change under those transformations. Therefore, general relativity relies on the invariance of the line element.

In quantum field theory, matter wave functions and interaction fields are quantized, resulting into the exchange of virtual interaction particles that mediate the exertion of forces as local gauge transformations. An instructive simile is provided in Fig. 1. The Fraser illusion in Fig. 1(a) can be interpreted by the interaction of the concentric twisted cord circles (representing Schrödinger wave functions) with the checkerboard background (i.e. the visual gauge field). The black and white shapes of the background interact with the twisted black and white sections of the circles in such a way, that the visual system interprets those patterns coherently as “round squares” that are deformed under the action of visual gauge forces. By contrast, Fig. 1(b) displays the unit circle (dotted) together with its deformation (solid) obtained from locally gauging the metric of Euclidian space as in general

relativity (see Appendix for details).¹

In contrast to Larson’s (2012) metaphorical usage of musical forces, Mazzola (1990, 2002) provides a quite different analogy between music theory and modern (non-folk) physics. Mazzola was probably the first who saw the close analogy between physics and music in connection with the existence of symmetries. In music, especially for the domain of modulation:

As force of transformation acts the instrument of modulation. The localization of “particles” is realized by means of the cadence of modulation. This kind of description is not unfamiliar to musicology: Schönberg, Uhde, and many others speak in a vague sense about forces between musical structures in order to explain musical changes in a comprehensible way. (Mazzola 1990, p. 200; our translation)

In order to codify Schönberg’s (1978) modulation theory, Mazzola (1990) invented the “modulation quantum” as a set of chords mediating musical transposition from one key into another key as a symmetry operation through exchange during cadences. Although we do not consider the domain of modulation in the present study, Mazzola’s insights are of highest importance for our work. As the central problem of our investigation we investigate the issue of tonal attraction. Our conception sees a close relationship between the phenomenon of tonal attraction and the existence of tonal forces. We therefore elucidate and reconcile musical forces in the framework of quantum cognition approaches which thereby lead to a precise and non-metaphorical understanding of musical forces. Our proposed model also presents a unifying account to the distinction between structural (Lerdahl and Jackendoff 1983, Lerdahl 1988) and probabilistic approaches (Temperley 2007, 2008) in computational music theory.

The paper is structured as follows: In the next section 2 we present, after a brief recapitulation of the essential concepts of music theory, two

¹ Unfortunately, we were not able to convert our quantum deformation into a corresponding Fraser illusion.

tonal attraction experiments of Krumhansl and Kessler (1982) on static attraction and of Woolhouse (2009) on dynamic attraction. Section 3 reports our theory for modeling these results. For the static attraction data we first review the classical hierarchical models of tonal space (Lerdahl 1988, 1996, Krumhansl and Kessler 1982, Krumhansl and Cuddy 2010) (for other models, cf. Temperley (2007, 2008), Stolzenburg (2015)). Second, we present two quantum models based on the essential symmetries of the chromatic octave and its representation theory investigated in harmonic analysis. Also for the dynamic attraction data, we first review one particular model of tonal space, the interval cycle model of Woolhouse (2009) and Woolhouse and Cross (2010). Guided by this approach we subsequently develop our quantum model for dynamical attraction analogous to the static case. The following section 4 presents the results of our quantum models and of the canonical models for comparison. The paper closes with a discussion and a short conclusion of our main findings.

2. Material and methods

As this study is devoted to symmetries in quantum models of static and dynamic tonal attraction, we first give a brief introduction into mathematical musicology (Balzano 1980, Mazzola 1990, 2002, Mazzola et al. 2016).

2.1. Elements of music

It is well known since Hermann von Helmholtz' (1877) groundbreaking studies that the human auditory system cannot distinguish between acoustic stimuli with pitch frequencies f_0, f_1 when their frequency ratios are separated by one octave: $f_1/f_0 = 2$. Hence octave equivalence induces an equivalence relation of acoustic stimuli into *pitch classes*, or *chroma* (Parncutt 2011) which circularly wind up throughout different octaves. Western music (among that of many other cultures) divides this continuous pitch class circle into twelve distinguished tones, or *degrees*, comprising the chromatic scale shown in Tab. 1.

interval j	0	1	2	3	4	5	6	7	8	9	10	11	12
tone	C	C \sharp	D	E \flat	E	F	F \sharp	G	A \flat	A	B \flat	B	C'

Table 1: Pitch classes as chromatic scale degrees.

Only a subset of seven tones that are arranged in a particular order of full-tone (major second) and semitone (minor second) steps comprise the *diatonic scales* of tonal music. For the key of C major, these are the seven tones in ascending order C, D, E, F, G, A, B, C', namely the white keys of a piano keyboard with C' closing the octave. The *tonic* C is regarded as the most stable note. The same tones arranged after cyclic permutation, A, B, C, D, E, F, G, A', entail the *relative minor* scale of (natural) A minor with tonic A.

Figure 2(a) presents the chroma circle (Krumhansl 1979) consisting of the twelve circularly repeating pitch classes of the chromatic scale in equal temperament, together with the C major scale degrees depicted as open bullets. The tonic C is indicated by $j = 0$. The relative A minor scale is obtained by rotating all tones 3 semitone steps (i.e. a minor third) in clockwise direction, thus assigning A to $j = 0$. The particular order: 2, 2, 1, 2, 2, 2, 1 of major second (2 steps) and minor second (1 step) intervals characterizes the major scale mode, while (natural) A minor is characterized by the interval order 2, 1, 2, 2, 1, 2, 2, as every other minor scale mode, too. Hence, the *parallel minor* scale of C major is (natural) C minor, comprising C, D, E \flat , F, G, A \flat , B \flat , C' with tonic C.

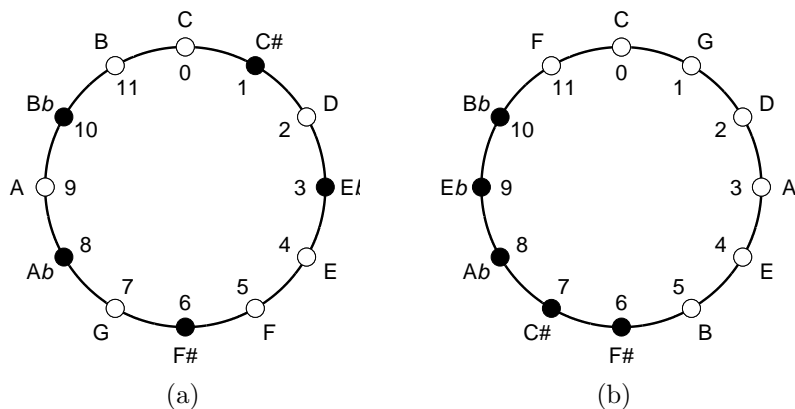


Figure 2: Tonal spaces of Western music. (a) Chroma circle of C major scale. (b) Circle of fifths. Open bullets indicate scale (diatonic) tones; closed bullets denote non-scale (chromatic) tones.

The chroma circle Fig. 2(a) exhibits the geometric symmetry of a dodecagon, corresponding to the cyclic group of integer cosets modulo twelve, \mathbb{Z}_{12} (Balzano 1980, Mazzola et al. 2016), that is generated by the semitone step $g \in \mathbb{Z}_{12}$ through its powers $g, g^2, g^3, \dots, g^{11}, g^{12}$ with $g^{12} = e$ as the neutral element of the group. Hence, the inverse of an element g^k is given as g^{12-k} with g^6 as its own inverse, i.e. g^6 is nilpotent. The application of the generator $g \in \mathbb{Z}_{12}$ to the chroma circle corresponds to a clockwise transposition by one semitone in Fig. 2(a).

The cyclic group \mathbb{Z}_{12} does not only possess the fundamental generator g . Yet all (integer) powers of g that are relatively prime with the group order $n = 12$ are generators as well. Therefore, we obtain all generators of \mathbb{Z}_{12} as $G_{12} = \{g, g^5, g^7, g^{11}\}$. As g corresponds to one semitone step in clockwise direction around the chroma circle, its inverse $g^{11} = g^{12-1}$ denotes one semitone step in counterclockwise direction. Similarly, g^7 in clockwise direction is inverse to g^5 in counterclockwise direction. Iterating the generator g^7 in clockwise direction to Fig. 2(a), i.e. by applying powers of $(g^7)^m$ to the tonic, yields the important *circle of fifths*, shown in Fig. 2(b), where all diatonic degrees are accumulated in a connected set (Balzano 1980). With the tonic of C major in position $j = 0$, its *dominant* G is in position $j = 1$, and its *subdominant* F is in position $j = 11$.

The crucial symmetry in tonal music is *transposition invariance* (Köhler 1969): A melody does not significantly alter its character, when played in a different key. Transposition from one key into another one is carried out by rotations either along the chroma circle or along the circle of fifths. Rotating all tones one step in clockwise direction, assigns $j = 0$ to F which thereby becomes the tonic of F major with dominant $j = 1$ at C and subdominant $j = 11$ at B \flat . Correspondingly, G major is obtained by a counterclockwise rotation by one step with tonic G ($j = 0$), dominant D ($j = 1$), and subdominant C ($j = 11$).

These are only a few examples for symmetries of the chroma circle. Others are the dichotomy between consonances and dissonances (Mazzola et al. 2016), or the emergence of the *third torus* as the direct group product $\mathbb{Z}_{12} = \mathbb{Z}_3 \times \mathbb{Z}_4$ (Balzano 1980, Mazzola et al. 2016) which is crucial for the canonical construction of chords in harmony theory (Schönberg 1978). This decomposition maps both, the chroma circle and the circle of fifths onto a torus, generated by a minor third (3 steps) in one direction and a major third (4 steps) in the orthogonal direction. Starting with C and going 4 steps, yields E, from where one arrives at G after 3 orthogonal steps, thus forming the C major triad CEG. Iterating first 3 and then 4 steps, instead, entails the C minor triad C \flat EG. Likewise, the F major triad is comprised by its tonic F, its major third, A, and the minor third C of A. For G major, one obtains correspondingly GBD.

2.2. Static tonal attraction

In a celebrated probe tone experiment on static tonal attraction, Krumhansl and Kessler (1982) asked musically experienced listeners to rate how well, on a seven point scale, each note of the chromatic octave fitted with a preceding context, which consisted of short musical sequences, such as ascending scales, chords, or cadences, in major or minor keys. All stimuli were prepared as artificial Shepard tones (Krumhansl and Kessler 1982, Woolhouse 2009, Milne et al. 2015), i.e. superpositions of pure sinusoids over five octaves with Gaussian amplitude envelopes.

The empirical results of Krumhansl and Kessler (1982) are replicated in Fig. 3 as dotted curves connecting open and closed bullets. The probe tones

are given as physical pitch frequencies (in Hz) at the x -axis. The subjective attraction ratings $A_{KK}(x)$ (referring to Krumhansl and Kessler) are plotted at the y -axis. Figure 3(a) shows the results for the C major context, and Fig. 3(b) for the C minor context. The results of this experiment clearly show a kind of hierarchy: all diatonic scale tones (open bullets) received higher ratings than the chromatic nonscale tones (closed bullets). Moreover, in both modes, C major and C minor, the tonic C is mostly attractive, followed by the fifth, G and the third E for C major [3(a)] and by the third Eb and then the fifth G for C minor [3(b)].

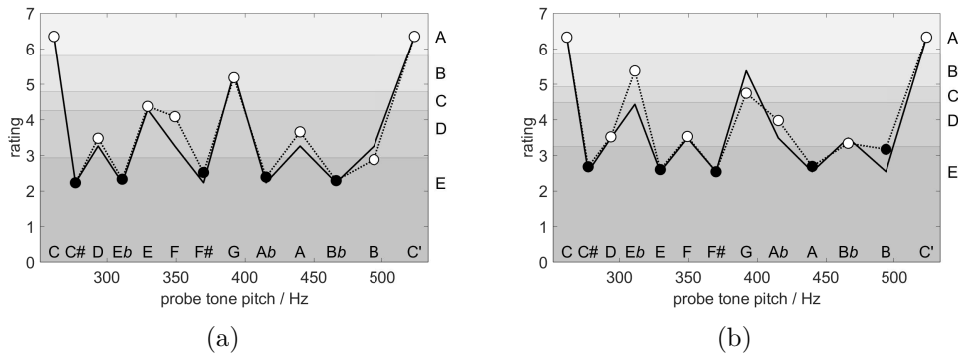


Figure 3: Static tonal attraction. Dotted with bullets: rating data $A_{KK}(x)$ of Krumhansl and Kessler (1982) against physical pitch frequency f in Hz, solid: Predictions from the hierarchical model [Eq. (1)]. The labels A – E at the right hand side indicate the labels of the hierarchical model [Tab. 2]. (a) For C major context. (b) For C minor context. Open bullets indicate scale (diatonic) tones; closed bullets denote non-scale (chromatic) tones, for the respective scale.

Carrying out a multiscale analysis of their behavioral data, Krumhansl and Kessler (1982) recovered a geometric representation of keys akin to the third torus, thereby supporting the hierarchical models of tonal space as discussed in Sect. 3.1.1 (Lerdahl 1988, 1996, Krumhansl and Kessler 1982, Krumhansl and Cuddy 2010). We additionally present the predictions of the hierarchical model as the solid curves together with the labels of its levels in Fig. 3.

2.3. Dynamic tonal attraction

Using five different chords, also consisting of Shepard tones, the C major triad CEG, the C minor triad CE \flat G, the dominant seventh CEG \flat B \flat , a

French sixth $CEG\flat B\flat$, and a half-diminished seventh $CE\flat G\flat B\flat$, as contexts, Woolhouse (2009) conducted a dynamic attraction probe tone experiment, asking listeners, how well a chromatic probe tone was melodically completing or harmonically resolving the priming context.

The results of this study are replicated in Sect. 4.2, Fig. 9 for the five contexts. The dotted curves connecting open and closed bullets present the original results of the Woolhouse (2009) experiment, where probe tones are arranged along the circle of fifths [Fig. 2(b)] as real numbers $x = j\pi/6$ ($j \in \mathbb{Z}_{12}$, with $C(0) \cong C'(12)$ one octave higher) at the x -axis.

Figure 9(a) displays the results for the C major priming context. The highest rated tone is F which is consistent with the interpretation of the priming C major triad as the dominant of F major. Another plausible interpretation of the prime would be the subdominant of G major, thus predicting higher likelihood of probe tone G. Similar results could be expected for the C minor context shown in Fig. 9(b). In fact, F receives a relatively large rating, however, outperformed by $A\flat$. Figure 9(c) displays the dominant seventh chord which is similar to the C major triad. The data for the French sixth presented in Fig. 9(d) give highest ratings for F and B and lowest ratings for D and $A\flat$. Finally, the half-diminished seventh [Fig. 9(e)] is most likely resolved by F, $C\sharp$ and B.

3. Theory

In this section we develop our quantum models of static and dynamic tonal attraction, based on the fundamental musical transposition symmetry.

3.1. Static tonal attraction

Before we enter into the derivation of two possible quantum models for static tonal attraction, we briefly review the influential symbolic model based on the generative theory of tonal music (Lerdahl and Jackendoff 1983).

3.1.1. Hierarchical model

The hierarchical model of Lerdahl (1988, 1996), Krumhansl and Kessler (1982), and Krumhansl and Cuddy (2010), depicted in Tab. 2, comprises five levels of symbolic significance.

A: octave	C												C'
B: fifths	C						G						C'
C: triadic	C			E			G						C'
D: diatonic	C		D	E	F		G		A		B		C'
E: chromatic	C	C \sharp	D	E \flat	E	F	F \sharp	G	A \flat	A	B \flat	B	C'
$s(j)$	4	0	1	0	2	1	0	3	0	1	0	1	4

Table 2: Hierarchical model of static tonal attraction for C major context after Lerdahl (1996, 2015).

At the lowest, chromatic level E, all 12 tones of the chromatic octave are included. At the next, the diatonic level D, only the diatonic scale degrees are represented. One level higher, at the triadic level C, the three tones composing the triad according to major and minor third steps along the third torus are present. Again, one level higher, only tonic and fifths comprise the fifths level B. At the highest octave level A, eventually only the tonic prevails. The levels A – E are indicated in Fig. 3 as four shades of grey.

For each chromatic scale degree that serves as probe tone in the Krumhansl and Kessler (1982) experiment, one simply counts the number of degrees that are commonly shared across levels A to D (omitting level E that is common for all tones). The resulting number, $s(j)$, for probe tone $j \in \mathbb{Z}_{12}$ can be related to an attraction probability (Temperley 2008)

$$p(j) = \frac{s(j)}{\sum_j s(j)} \quad (1)$$

that is rescaled and plotted in Fig. 3 above as solid lines and correlated with the Krumhansl and Kessler (1982) data in Tab. 5 in Sect. 4.1.²

² For C minor we use the so-called *natural* minor scale which is obtained from the

The predictions of the hierarchical model are in good agreement with the experimental data. However, Fig. 3(b) indicates a slight deviation for C minor: the predicted attraction rate for the fifths G is larger and that of the minor third Eb is lower than the respective measured rate. We address this issue in section 3.1.5 below.

3.1.2. Free quantum model

A more instructive representation of the Krumhansl and Kessler (1982) data can be obtained by plotting the ratings $A_{KK}(x)$ along the circle of fifths. This is done in Sect. 4.1, Fig. 6. Here, the probe tones are represented as real numbers $x = j\pi/6$ ($j \in \mathbb{Z}_{12}$, with $C(0) \cong C'(12)$ one octave higher) at the x -axis corresponding to the radian angles at the unit circle $S^1 = \mathbb{R}/2\pi\mathbb{Z}$ interpreted as the circle of fifths [Fig. 2(b)]. The subjective attraction ratings $A_{KK}(x)$ are plotted at the y -axis. Figure 6(a) shows the results for the C major context, and 6(b) for the C minor context.

The reordered rating profiles in Fig. 6 now exhibit some kind of periodicity: probe tones that are close to the tonic C ($x = 0$) at the circle of fifths receive higher attraction values than tones that are close to the tritone F \sharp ($x = \pi$). Therefore, the tritone F \sharp may be seen as “orthogonal” to the tonic C in an appropriately chosen metric (cf. Mannone and Compagno (2013), Mannone and Mazzola (2015) for alternative similarity assessments in musicology). A suitable choice is therefore given as cosine similarity between the tonic context 0 and a probe tone x ,

$$p(x) = \cos^2 \frac{x}{2}. \quad (2)$$

Cosine similarity is closely related to quantum similarity (Pothos et al. 2013, Pothos and Trueblood 2015) in the framework of quantum cognition models (Busemeyer and Bruza 2012, Pothos and Busemeyer 2013, Blutner and beim Graben 2016). Therefore, we express the attraction value $p(x)$ through a continuous “wave function” $\psi(x)$ upon the circle of fifths which constitutes the one-

transposition of C major along the circle of fifths. There are two other minor scales, called *harmonic* and *melodic* minor which differ from natural minor in additional one or two semitone steps in ascending or descending lines.

dimensional “tonal configuration space” of our quantum model.³

Quantum mechanical wave functions are particular instances of *state vectors* in quantum theory. A state vector comprises a complete description of the state of a quantum system. It is contained in a vector space, called Hilbert space, that is equipped with a scalar product, thus allowing the calculation of projections. A quantum mechanical measurement device defines an orthogonal basis, such that the projections of a given state vector onto the individual basis vectors are interpreted as probabilities of the respective measurement results. Accordingly is the similarity of two quantum states given through the projection of one vector onto the other one, i.e. their common scalar product. Moreover, rotating a state vector in abstract Hilbert space must not change its physically relevant properties, i.e. projection probabilities. Therefore such rotations appear as *symmetries* in quantum theory.

Our *free quantum model* for the tonic wave function is hence

$$\psi(x) = \frac{1}{\sqrt{\pi}} \cos \frac{x}{2}. \quad (3)$$

Differentiating (3) twice yields an ordinary differential equation of second order

$$\begin{aligned} \psi'(x) &= -\frac{1}{2\sqrt{\pi}} \sin \frac{x}{2} \\ \psi''(x) &= -\frac{1}{4\sqrt{\pi}} \cos \frac{x}{2} \\ -\psi''(x) &= \frac{1}{4}\psi(x) \end{aligned} \quad (4)$$

which can be interpreted as an eigenvalue equation

$$T\psi(x) = E\psi(x) \quad (5)$$

for the differential operator

$$T = -\frac{\partial^2}{\partial x^2} \quad (6)$$

³ Note that the unit circle S^1 is a one-dimensional manifold, parameterized by a single continuous variable $x \in [0, 2\pi[$, that is embedded into two-dimensional Euclidian space.

with eigenvalue $E = 1/4$. Written in the form (5), (4), turns out to be the quantum mechanical stationary Schrödinger equation for the motion of a “free-particle” with kinetic energy $E = 1/4$. The operator T must therefore be interpreted as the operator of *inertia* or kinetic energy.

The stationary Schrödinger equation in the form (5) provides the quantum probability amplitudes for time-independent problems in quantum theory. It is closely related to the stationary probability distribution given as the positive eigenvector for eigenvalue one of a Markov transition matrix in the theory of Markov processes. Therefore, quantum approaches to music cognition embrace classical probabilistic accounts such as Bayesian modeling or Markov processes (Temperley 2007, 2008).

The quantum similarity function (2) for an arbitrary context tone a is obtained by applying a transposition operator T_a to the tonic context 0 through

$$\psi_a(x) = T_a\psi(x) = \psi(x - a) \quad (7)$$

for the amount a rotating along the circle of fifths in clockwise direction. Note that the subscript a of T_a must be regarded as an element of the transposition symmetry group \mathbb{Z}_{12} , while a in the wave function’s argument becomes an element of the configuration space S^1 . Thus, we have to consider the representation theory of the musical transposition symmetry on the Hilbert space of wave functions over the configuration space. Such representations are subject of the mathematical discipline of *harmonic analysis*. For admissible musical transpositions, the lag a is taken from the cyclic group \mathbb{Z}_{12} . However, in the general framework of harmonic analysis it is more appropriate to consider continuous transposition symmetry, described by the circle group $U(1)$ here. In section 3.1.3 below we demonstrate how the particularly discrete structure of tonal space emerges from musical transposition symmetry under additional assumptions about the interaction of multiple context tones within chords. The significance of symmetry principles indicates how our quantum approach also embraces structural aspects of music cognition (Lerdahl and Jackendoff 1983, Lerdahl 1988). In this sense, our approach unifies both, structural and probabilistic accounts for computational music theory, in a broader framework.

Applying the transposition operator to the tonic wave function (3), we

obtain

$$\psi_a(x) = \frac{1}{\sqrt{\pi}} \cos \frac{x-a}{2} \quad (8)$$

which can be expanded by virtue of the trigonometric addition theorems:

$$\begin{aligned} \psi_a(x) &= \frac{1}{\sqrt{\pi}} \cos \frac{x-a}{2} \\ &= \frac{1}{\sqrt{\pi}} \cos \frac{a}{2} \cos \frac{x}{2} + \frac{1}{\sqrt{\pi}} \sin \frac{a}{2} \sin \frac{x}{2} \\ &= \frac{1}{\sqrt{\pi}} \cos \frac{a}{2} \cos \frac{x}{2} + \frac{1}{\sqrt{\pi}} \sin \frac{a}{2} \cos \frac{x-\pi}{2} \\ &= \cos \frac{a}{2} \psi_0(x) + \sin \frac{a}{2} \psi_\pi(x). \end{aligned}$$

Hence any transposed state becomes a linear combination of two basic context states, the tonic (C) ψ_0 , and the orthogonal tritone (F \sharp) ψ_π . The underlying Hilbert space of the free quantum model is therefore two-dimensional which proves the equivalence of this model with the earlier qubit model of Blutner (2015). Moreover, the transposition operator T_a becomes hence represented as a unitary operator in Hilbert space.

The family $\{\psi_0, \psi_\pi\}$ constitutes an orthonormal basis with respect to the wave function scalar product

$$\langle \psi_y | \psi_a \rangle = \int_0^{2\pi} \psi_y(x)^* \psi_a(x) dx \quad (9)$$

where complex conjugation can be essentially neglected in the present case. Inserting the respective transposed wave functions yields

$$\begin{aligned} \langle \psi_y | \psi_a \rangle &= \left\langle \cos \frac{y}{2} \psi_0 + \sin \frac{y}{2} \psi_\pi \left| \cos \frac{a}{2} \psi_0 + \sin \frac{a}{2} \psi_\pi \right. \right\rangle \\ &= \cos \frac{y}{2} \cos \frac{a}{2} \langle \psi_0 | \psi_0 \rangle + \cos \frac{y}{2} \sin \frac{a}{2} \langle \psi_0 | \psi_\pi \rangle + \sin \frac{y}{2} \cos \frac{a}{2} \langle \psi_\pi | \psi_0 \rangle + \sin \frac{y}{2} \sin \frac{a}{2} \langle \psi_\pi | \psi_\pi \rangle \\ &= \cos \frac{y}{2} \cos \frac{a}{2} + \sin \frac{y}{2} \sin \frac{a}{2} \\ &= \cos \frac{y-a}{2} \end{aligned}$$

which is, up to a scaling factor,

$$\langle \psi_y | \psi_a \rangle = \sqrt{\pi} \psi(y-a), \quad (10)$$

the original wave function for the interval between probe tone y and context tone a . Therefore, we can use the (scaled) quantum probability density

$$p(x) = |\psi(x)|^2 = \psi(x)^* \psi(x) \quad (11)$$

for a given interval as a measure of tonal attraction $p(y - a)$.

Sofar, our wave functions yield static tonal attraction values through the projection (10) of a probe tone state onto a context tone state. In order to describe chord contexts, Woolhouse (2009), Woolhouse and Cross (2010) and Blutner (2015) suggested either to sum or to average the attraction profiles of individual pairs of tones over all pairings. For a context of two tones a, b this *Woolhouse conjecture* yields

$$p_{ab}(x) = |\psi_{ab}(x)|^2 = \frac{1}{2} (|\psi_a(x)|^2 + |\psi_b(x)|^2) , \quad (12)$$

in analogy to the density matrix formalism of statistical quantum mechanics (cf. Mannone (2018) for a related account in musicology). For an arbitrary number N of equally weighted context tones in a chord, we get

$$p_C(x) = \frac{1}{N} \sum_{i=1}^N |\psi_{a_i}(x)|^2 = \frac{1}{N} \sum_{i=1}^N |\psi(x - a_i)|^2 \quad (13)$$

with context $C = \{a_i \in S^1 | i = 1, \dots, N\}$. When context tones are to be considered as differently weighted, we introduce weight factors $\rho(a_i)$ (Mazzola 2002) and obtain a discrete convolution

$$p_C(x) = \sum_{i=1}^N \rho(a_i) p(x - a_i) \quad (14)$$

with kernel $p(x) = |\psi(x)|^2$. Yet, we only use equally weighted contexts $\rho(a_i) = 1/N$ in our present exposition.

3.1.3. Quantum deformation model

The data of the Krumhansl and Kessler (1982) experiment as shown in Sect. 4.1, Fig. 6 and their spatial reconstruction through our free quantum

model in Sect. 3.1.2 demonstrate that music cognition is based on geometrically represented tonal space (Lerdahl 1988, Krumhansl and Kessler 1982, Janata 2007). In this subsection, we show how a straightforward modification of the free model leads to a more parsimonious representation theory of tonal space than the hierarchical model discussed in Sect. 3.1.1.

To this aim, we introduce a suitable deformation of the distances along the circle of fifths by making the ansatz

$$\psi(x) = A \cos(\gamma(x)) \quad (15)$$

for the stationary wave function where $\gamma(x)$ is a spatial deformation function and A a normalization constant.

Before we derive the particular deformation for the Krumhansl and Kessler (1982) data, it is instructive to consider the generic case of an arbitrary deformation function $\gamma(x)$. Differentiating (15) twice yields

$$\begin{aligned} \psi'(x) &= -A\gamma'(x) \sin(\gamma(x)) \\ \psi''(x) &= -A\gamma''(x) \sin(\gamma(x)) - A\gamma'(x)^2 \cos(\gamma(x)). \end{aligned}$$

Eliminating trigonometric terms, we then obtain the differential equation

$$-\psi''(x) + \frac{\gamma''(x)}{\gamma'(x)}\psi'(x) - \gamma'(x)^2\psi(x) = 0 \quad (16)$$

which we compare with the general stationary Schrödinger equation $H\psi(x) = E\psi(x)$ for energy eigenvalue E . With

$$H = T + M + U \quad (17)$$

this comparison yields the following operators: The first term T is the operator of kinetic energy (6), again. The second term could be interpreted as *magnetic interaction energy* which involves the first derivative of the wave function⁴

$$M = \frac{\gamma''(x)}{\gamma'(x)} \frac{\partial}{\partial x}. \quad (18)$$

⁴ See Appendix for details of the derivation.

The ratio $\gamma''(x)/\gamma'(x)$ plays here the role of the magnetic vector potential. Finally, the last term, which is simply a scalar multiplication operator, receives its usual interpretation as potential energy

$$U = E - \gamma'(x)^2 \tag{19}$$

which might be seen as *gravitational potential*. In an earlier study, we have outlined a local gauge theory of these forces (beim Graben and Blutner 2017). Note that only the physical interpretation suggests the notions of “inertia”, “magnetism”, or “gravity” for the emergent terms in the Schrödinger equation (16). They are not at all related to the metaphorical intuitions in musicology, inspired by interpreting these concepts in terms of folk-physics (Larson and van Handel 2005, Larson 2012). We leave the clarification of their musicological meaning for future research.

In order to interpret the constant E , we connect our results to the free model of Sect. 3.1.2, for which $M = 0$ and $U = 0$ must hold, i.e. neither magnetic nor gravitational forces are exerted on the “free particle”. First, $M = 0$ implies

$$\begin{aligned} \gamma''(x) &= 0 \\ \gamma'(x) &= a_1 \\ \gamma(x) &= a_0 + a_1x \end{aligned}$$

where the integration constants must obey the interpolation equations

$$\begin{aligned} \gamma(0) &= 0 \\ \gamma(\pi) &= \frac{\pi}{2}, \end{aligned}$$

yielding $a_0 = 0$ and $a_1 = 1/2$, thereby rendering the free model above. Second, $U = E - \gamma'(x)^2 = 0$ for all $x \in S^1$ implies

$$E = \gamma'(0)^2 \tag{20}$$

in particular. Hence, $E = a_1^2 = 1/4$ in agreement with the free Schrödinger equation (4).

3.1.4. Symmetric deformation

Now we are prepared to develop the deformation model for the Krumhansl and Kessler (1982) data. First, we linearly rescale the empirical data

$$A_{\text{KK}}(x) = ap(x) + b. \quad (21)$$

Inserting scaling constants $a = A_{\text{max}} - A_{\text{min}}$, $b = A_{\text{min}}$, where A_{min} and A_{max} are the smallest and largest data values, and Eq. (15), and subsequently solving for γ yields

$$\gamma(x) = \arccos \sqrt{\frac{A_{\text{KK}}(x) - A_{\text{min}}}{A_{\text{max}} - A_{\text{min}}}}. \quad (22)$$

When we transform the C major data according to (22) we obtain $\gamma(x)$ as the dotted curve in Fig. 4(a) resembling a buckled parabola (though neglecting the peak at E). Thus, we fit the exponent n of a symmetric n -th order polynomial

$$\gamma(x) = a_0 + a_n(x - \pi)^n, \quad (23)$$

to the transformed data. For $n = 2$ the fit is rather poor ($r = 0.88$) and not really able to reproduce the buckle in the transformed data set. The next fit $n = 4$ works considerably well ($r = 0.96$), while exponents of higher than fourth order ($n = 6, 8$) do not substantially improve our fits. Thus, our choice $n = 4$ fits the data most parsimoniously.

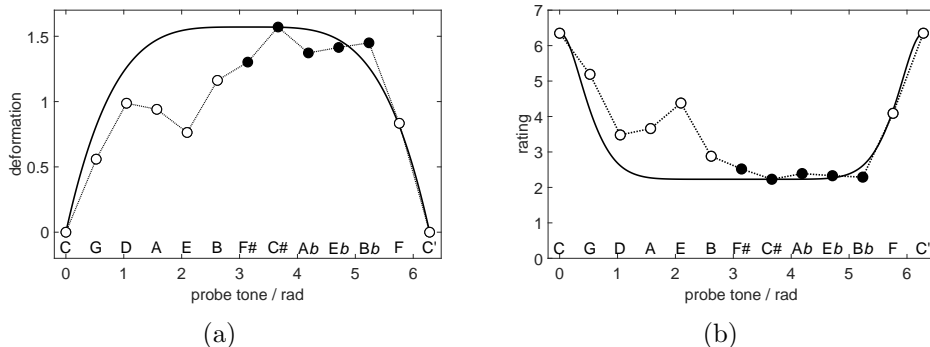


Figure 4: Optimal deformation of the cosine similarity profile for static tonal attraction. (a) Transformed Krumhansl and Kessler (1982) data [Eq. (22)] (dotted) against radian angles at the circle of fifths and deformation function (24) (solid). (b) Rating data $A_{\text{KK}}(x)$ of Krumhansl and Kessler (1982) (dotted) and quantum probability kernel Eq. (11) (solid). Both for C major context.

The two parameters a_0, a_4 are necessarily obtained from two interpolation equations

$$\begin{aligned}\gamma(0) &= 0 \\ \gamma(\pi) &= \frac{\pi}{2},\end{aligned}$$

i.e. the tonic should not be deformed while the tritone receives maximal deformation, as reflected by Fig. 4(a). Note that we do not perform a least-square fit for the parameters by minimizing some error functional. The parameters are fixed by the constraint that the deformation function should vanish at C and assume a maximum at F♯. This leads to the parsimonious parameter-free model

$$\gamma(x) = \frac{\pi}{2} - \frac{(x - \pi)^4}{2\pi^3}. \quad (24)$$

We plot the original Krumhansl and Kessler (1982) data and the quantum probability density kernel (11) of the deformation model (15) in Fig. 4(b). At this point, it is useful to ask for the connection between the deformation model and the hierarchical model. As one sees from Fig. 4(b), the kernel function of (static) tonal attraction assigns the maximum value to the target tone (say C). The two neighbors on the circle of fifth (i.e., G and F) get an attraction value that is about half of it. The attraction values of all other tones is very low such that we can neglect them. Hence, when we construct the attraction profiles for a certain context given by a triad (say CEG), we get an approximate reconstruction of the hierarchic model. The three tones of the triad (CEG) get a very high value; C and G a bit higher than E because of the convolution operation. Next, the neighbors of the triadic tones (C'G,F vs. G'D,C vs. E'B,A) are all diatonic tones and get an attraction of about 50%. Hence, we can account for all levels of the hierarchic model shown in Tab. 2 besides the octave level (resulting in 4 different degrees of attraction).

The Schrödinger equation of the deformation model obeys conservation of energy, as unveiled by multiplication with the adjoint solution ψ^* from the left. Introducing energy densities

$$T(x) = -\psi(x)^* \psi''(x) \quad (25)$$

$$M(x) = \psi(x)^* \frac{\gamma''(x)}{\gamma'(x)} \psi'(x) \quad (26)$$

$$U(x) = \psi(x)^* (E - \gamma'(x)^2) \psi(x) \quad (27)$$

yields

$$T(x) + M(x) + U(x) = E\psi(x)^*\psi(x) = Ep(x)$$

with $p(x) = |\psi(x)|^2$ the resulting probability distribution. Interestingly, this distribution describes the original Krumhansl and Kessler (1982) data which therefore receive a straightforward interpretation as *total energy density* of tonal attraction.

Given the potential energy densities $M(x)$ and $U(x)$, we compute the corresponding forces as their negative gradients

$$F_M(x) = -M'(x) \tag{28}$$

$$F_U(x) = -U'(x) \tag{29}$$

and also the resultant

$$F(x) = F_M(x) + F_U(x) \tag{30}$$

for a “bounded particle” with $E = 0$.

Next, we discuss the structure of the Hilbert space of the quantum deformation model. We show here that the quantum deformation model requires the infinite-dimensional Hilbert space of Fourier series over the unit circle. Combining this with the condition of transposition symmetry leads to a discrete system of musical tones, thereby excluding a tonal continuum that could be possible from acoustic pitch frequencies. Hence, we offer a solution to one of the big mysteries of tonal music: Why do we find discrete tonal systems in human music contrasting with other tonal systems, for example of bird songs (Araya-Salas 2012). Moreover, we solve the superposition problem for chord contexts. The data indicate that tonal quantum states do not linearly superimpose but rather mix up in density matrices. However, this mixing hypothesis is consistent with a superposition law for interacting musical forces.

In order to understand the Hilbert space structure, we rewrite the Schrödinger equation (16) as

$$-\psi''(x) + m(x)\psi'(x) + g(x)\psi(x) = 0 \tag{31}$$

with “magnetic”

$$m(x) = \frac{\gamma''(x)}{\gamma'(x)}, \tag{32}$$

and “gravitational” interaction energies

$$g(x) = -\gamma'(x)^2. \quad (33)$$

Since the functions m, g, ψ are defined on the configuration space of the unit circle (viz the circle of fifths), they obey its circular symmetry and must hence be 2π -periodic functions over \mathbb{R} . Thus in the framework of harmonic analysis, we develop them into their Fourier series (if they exist):

$$m(x) = \sum_k M_k e^{ikx} \quad (34)$$

$$g(x) = \sum_k G_k e^{ikx} \quad (35)$$

$$\psi(x) = \sum_k P_k e^{ikx} \quad (36)$$

where the indices extend over all integers $-\infty < k < \infty$. The Fourier coefficients are given as

$$M_k = \frac{1}{2\pi} \int_0^{2\pi} m(x) e^{-ikx} dx \quad (37)$$

$$G_k = \frac{1}{2\pi} \int_0^{2\pi} g(x) e^{-ikx} dx \quad (38)$$

$$P_k = \frac{1}{2\pi} \int_0^{2\pi} \psi(x) e^{-ikx} dx. \quad (39)$$

Inserting (34 – 36) into the original Schrödinger equation (31) yields its equivalent in Fourier space

$$k^2 P_k + \sum_l (ilM_{k-l} + G_{k-l}) P_l = 0 \quad (40)$$

that must be solved for all $k, l \in \mathbb{Z}$. For given magnetic and gravitation force terms M_k, G_k , there will be in general an infinite number of solution coefficients P_k , such that the Hilbert space of the quantum deformation model is also infinite-dimensional, in contrast to the two-dimensional Hilbert space of the free quantum model, discussed in section 3.1.2. For numerical solutions, we approximate the Fourier series by the leading eleven terms of the corresponding cosine series.

First, we prove that musical transposition symmetry holds also in Fourier space. To this end, we recognize that a (continuous) transposition $a \in [0, 2\pi[$ turns out to be equivalent with multiplication by a constant phase factor, i.e. a gauge transformation of every individual Fourier mode (beim Graben and Blutner 2017):

$$m(x - a) = \sum_k M_k e^{ik(x-a)} = \sum_k M_k e^{ikx} e^{-ika} \quad (41)$$

$$g(x - a) = \sum_k G_k e^{ik(x-a)} = \sum_k G_k e^{ikx} e^{-ika} \quad (42)$$

$$\psi(x - a) = \sum_k P_k e^{ik(x-a)} = \sum_k P_k e^{ikx} e^{-ika} , \quad (43)$$

such that

$$m(x - a) = \sum_k \tilde{M}_k e^{ikx} \quad (44)$$

$$g(x - a) = \sum_k \tilde{G}_k e^{ikx} \quad (45)$$

$$\psi(x - a) = \sum_k \tilde{P}_k e^{ikx} \quad (46)$$

with

$$\tilde{M}_k = M_k e^{-ika} \quad (47)$$

$$\tilde{G}_k = G_k e^{-ika} \quad (48)$$

$$\tilde{P}_k = P_k e^{-ika} . \quad (49)$$

Replacing all Fourier coefficients M_k, G_k, P_k in (40) by the transposed ones in (47 — 49) yields then

$$\begin{aligned} k^2 \tilde{P}_k + \sum_l (i l \tilde{M}_{k-l} + \tilde{G}_{k-l}) \tilde{P}_l &= 0 \\ k^2 P_k e^{-ika} + \sum_l (i l M_{k-l} e^{-i(k-l)a} + G_{k-l} e^{-i(k-l)a}) P_l e^{-ila} &= 0 \\ k^2 P_k e^{-ika} + \sum_l (i l M_{k-l} + G_{k-l}) P_l e^{-ika} &= 0 \\ k^2 P_k + \sum_l (i l M_{k-l} + G_{k-l}) P_l &= 0 , \end{aligned}$$

i.e. continuous transposition invariance.

Finally, we address the mathematical consequences of the mixing conjecture (12)

$$p_{ab}(x) = |\psi_{ab}(x)|^2 = \frac{1}{2} (|\psi_a(x)|^2 + |\psi_b(x)|^2)$$

for interacting intervals $a, b \in C$ in a chordal context C . Because we were not able to specify any reasonable superposition law either for wave functions or for musical forces yet, we suggest a kind of “reverse engineering” approach here. Hence, we take the conjecture (12) for granted and derive a superposition law from the transposition invariance of the Schrödinger equation in Fourier space (40) next.

Under the assumption that the solution wave function ψ_{ab} has the Fourier series

$$\psi_{ab}(x) = \sum_k Q_k e^{ikx} \quad (50)$$

we obtain on the one hand

$$|\psi_{ab}(x)|^2 = \sum_{kl} Q_k Q_l^* e^{i(k-l)x}$$

for the convolution. On the other hand, we have

$$\begin{aligned} |\psi_a(x)|^2 &= \sum_{kl} P_k P_l^* e^{i(k-l)x} e^{-i(k-l)a} \\ |\psi_b(x)|^2 &= \sum_{kl} P_k P_l^* e^{i(k-l)x} e^{-i(k-l)b} \end{aligned}$$

due to Eq. (43). Their mixture yields then the identity

$$Q_k Q_l^* = \frac{1}{2} (e^{-i(k-l)a} + e^{-i(k-l)b}) P_k P_l^*. \quad (51)$$

In order to continue, we also need the complex conjugated Schrödinger equation

$$k^2 P_k^* + \sum_l (-ilM_{k-l}^* + G_{k-l}^*) P_l^* = 0 \quad (52)$$

such that the product of (40) and (52) yields

$$\begin{aligned}
& k^2 m^2 P_k P_m^* + k^2 \sum_n (-inM_{m-n}^* + G_{m-n}^*) P_k P_n^* + \\
& + m^2 \sum_l (ilM_{k-l} + G_{k-l}) P_l P_m^* + \sum_{ln} (ilM_{k-l} + G_{k-l}) (-inM_{m-n}^* + G_{m-n}^*) P_l P_n^* = 0.
\end{aligned} \tag{53}$$

Now we assume that the mixed wave function ψ_{ab} obeys a structurally similar product equation

$$\begin{aligned}
& k^2 m^2 Q_k Q_m^* + k^2 \sum_n (-in\hat{M}_{m-n}^* + \hat{G}_{m-n}^*) Q_k Q_n^* + \\
& + m^2 \sum_l (il\hat{M}_{k-l} + \hat{G}_{k-l}) Q_l Q_m^* + \sum_{ln} (il\hat{M}_{k-l} + \hat{G}_{k-l}) (-in\hat{M}_{m-n}^* + \hat{G}_{m-n}^*) Q_l Q_n^* = 0
\end{aligned} \tag{54}$$

in Fourier space, where \hat{M}_k, \hat{G}_k are the Fourier coefficients of the yet unknown superposition forces resulting from the interaction of two context tones a and b .

Inserting (51) into (54) gives

$$\begin{aligned}
& k^2 m^2 (e^{-i(k-m)a} + e^{-i(k-m)b}) P_k P_m^* + \\
& + k^2 \sum_n (-in\hat{M}_{m-n}^* + \hat{G}_{m-n}^*) (e^{-i(k-n)a} + e^{-i(k-n)b}) P_k P_n^* + \\
& + m^2 \sum_l (il\hat{M}_{k-l} + \hat{G}_{k-l}) (e^{-i(l-m)a} + e^{-i(l-m)b}) P_l P_m^* + \\
& \sum_{ln} (il\hat{M}_{k-l} + \hat{G}_{k-l}) (-in\hat{M}_{m-n}^* + \hat{G}_{m-n}^*) (e^{-i(l-n)a} + e^{-i(l-n)b}) P_l P_n^* = 0.
\end{aligned} \tag{55}$$

When $e^{-i(k-m)a} + e^{-i(k-m)b} \neq 0$, we can divide by this term and obtain

$$\begin{aligned}
& k^2 m^2 P_k P_m^* + k^2 \sum_n (-in \hat{M}_{m-n}^* + \hat{G}_{m-n}^*) \frac{e^{-i(k-n)a} + e^{-i(k-n)b}}{e^{-i(k-m)a} + e^{-i(k-m)b}} P_k P_n^* + \\
& \quad + m^2 \sum_l (il \hat{M}_{k-l} + \hat{G}_{k-l}) \frac{e^{-i(l-m)a} + e^{-i(l-m)b}}{e^{-i(k-m)a} + e^{-i(k-m)b}} P_l P_m^* + \\
& \quad \sum_{ln} (il \hat{M}_{k-l} + \hat{G}_{k-l}) (-in \hat{M}_{m-n}^* + \hat{G}_{m-n}^*) \frac{e^{-i(l-n)a} + e^{-i(l-n)b}}{e^{-i(k-m)a} + e^{-i(k-m)b}} P_l P_n^* = 0.
\end{aligned} \tag{56}$$

As all the fractions above are similar, we discuss their general form

$$F_{ab}(p, q) = \frac{e^{-ipa} + e^{-ipb}}{e^{-iqa} + e^{-iqb}} \tag{57}$$

for independent $p, q \in \mathbb{Z}$. First, we use Euler's formula for rewriting

$$e^{-ipa} + e^{-ipb} = 2 \cos \frac{p(a-b)}{2} \exp \left[-i \frac{p(a+b)}{2} \right]$$

and thus

$$F_{ab}(p, q) = \frac{\cos \frac{p(a-b)}{2}}{\cos \frac{q(a-b)}{2}} \exp \left[-i \frac{(p-q)(a+b)}{2} \right].$$

To evaluate the first term, we substitute $p - q = u$ and insert $p = u + q$ into the denominator

$$\cos \frac{p(a-b)}{2} = \cos \frac{u(a-b)}{2} \cos \frac{q(a-b)}{2} - \sin \frac{u(a-b)}{2} \sin \frac{q(a-b)}{2}$$

by virtue of the trigonometric addition theorems. Inserting this into F_{ab} again, yields

$$\begin{aligned}
F_{ab}(p, q) = & \cos \frac{(p-q)(a-b)}{2} \exp \left[-i \frac{(p-q)(a+b)}{2} \right] - \\
& - \sin \frac{(p-q)(a-b)}{2} \tan \frac{q(a-b)}{2} \exp \left[-i \frac{(p-q)(a+b)}{2} \right],
\end{aligned}$$

after reverting the substitution.

This function depends only on the interval $p - q$ if

$$\tan \frac{q(a - b)}{2} = 0 \tag{58}$$

for all $q \in \mathbb{Z}$. Moreover, the poles q_∞ of

$$\tan \frac{q_\infty(a - b)}{2} = \pm\infty \tag{59}$$

must be excluded in order to permit the division in Eq. (56).

We discuss these *quantization conditions* (Schrödinger 1926) in more detail. Consider (58) first, which holds for all $q \in \mathbb{Z}$ if there is another $p \in \mathbb{Z}$ with

$$q(a - b) = 2\pi p. \tag{60}$$

Because of the periodicity of (58), we choose p as a multiple of q , i.e. $p = jq$ with some $j \in \mathbb{Z}$.

Equation (60) is solvable in \mathbb{Z} only when the interval $a - b$ is a rational multiple of 2π . We therefore assume the existence of fixed integers $r, s \in \mathbb{Z}$ and $z \in \mathbb{N}$, such that $a = 2\pi r/z, b = 2\pi s/z$ and obtain

$$a - b = 2\pi \frac{r - s}{z}. \tag{61}$$

Inserting (61) into (60) yields

$$r - s = jz, \tag{62}$$

which means that r, s are congruent modulo z . Thereby $r, s \in \mathbb{Z}_z$ with the cyclic group \mathbb{Z}_z . For Western music we have particularly $z = 12$, and hence $a, b \in \frac{\pi}{6}\mathbb{Z}_{12}$. Thus, the originally assumed continuous transposition symmetry $U(1)$ breaks down into the cyclic group of the circle of fifths, leading to the emergence of the chromatic scale from musical transposition invariance. Note that the same argument also applies to contemporary approaches for microtonality which give rise to other cyclic groups \mathbb{Z}_z , with $z = 20, 30$, or $z = 42$ (Balzano 1980).

We proceed with Eq. (59) which means there is a $p \in \mathbb{Z}$ for each pole $q_\infty \in \mathbb{Z}$ with

$$q_\infty(a-b) = \pi + 2\pi p. \quad (63)$$

Inserting (61) into (63) shows that there cannot be integer poles $q_\infty \in \mathbb{Z}$ at all.

Thus, we are allowed to introduce a function

$$H_{ab}(z) = \cos \frac{z(a-b)}{2} \exp \left[-i \frac{z(a+b)}{2} \right] \quad (64)$$

which now appears in the Schrödinger product equation (56) as follows

$$\begin{aligned} & k^2 m^2 P_k P_m^* + k^2 \sum_n (-in \hat{M}_{m-n}^* + \hat{G}_{m-n}^*) H_{ab}(m-n) P_k P_n^* + \\ & \quad + m^2 \sum_l (il \hat{M}_{k-l} + \hat{G}_{k-l}) H_{ab}(l-k) P_l P_m^* + \\ & \sum_{ln} (il \hat{M}_{k-l} + \hat{G}_{k-l}) (-in \hat{M}_{m-n}^* + \hat{G}_{m-n}^*) H_{ab}(l-n-k+m) P_l P_n^* = 0, \end{aligned} \quad (65)$$

and after complex conjugation for $H_{ab}(l-k) = H_{ab}^*(k-l)$,

$$\begin{aligned} & k^2 m^2 P_k P_m^* + k^2 \sum_n (-in \hat{M}_{m-n}^* + \hat{G}_{m-n}^*) H_{ab}(m-n) P_k P_n^* + \\ & \quad + m^2 \sum_l (il \hat{M}_{k-l} + \hat{G}_{k-l}) H_{ab}^*(k-l) P_l P_m^* + \\ & \sum_{ln} (il \hat{M}_{k-l} + \hat{G}_{k-l}) (-in \hat{M}_{m-n}^* + \hat{G}_{m-n}^*) H_{ab}(l-n-k+m) P_l P_n^* = 0. \end{aligned} \quad (66)$$

Equations (53) and (66) lead to the following invariance constraints

$$\hat{M}_{m-n}^* H_{ab}(m-n) = M_{m-n}^* \quad (67)$$

$$\hat{G}_{m-n}^* H_{ab}(m-n) = G_{m-n}^* \quad (68)$$

$$\hat{M}_{k-l} H_{ab}^*(k-l) = M_{k-l} \quad (69)$$

$$\hat{G}_{k-l} H_{ab}^*(k-l) = G_{k-l} \quad (70)$$

$$\hat{M}_{k-l} \hat{M}_{m-n}^* H_{ab}(l-n-k+m) = M_{k-l} M_{m-n}^* \quad (71)$$

$$\hat{M}_{k-l} \hat{G}_{m-n}^* H_{ab}(l-n-k+m) = M_{k-l} G_{m-n}^* \quad (72)$$

$$\hat{G}_{k-l} \hat{M}_{m-n}^* H_{ab}(l-n-k+m) = G_{k-l} M_{m-n}^* \quad (73)$$

$$\hat{G}_{k-l} \hat{G}_{m-n}^* H_{ab}(l-n-k+m) = G_{k-l} G_{m-n}^* \quad (74)$$

Equations (67) and (69) are redundant, as (68) and (70) are as well. Thus, we use (69) and (70) for the deduction of the musical superposition forces:

$$\hat{M}_k = \frac{M_k}{H_{ab}^*(k)} \quad (75)$$

$$\hat{G}_k = \frac{G_k}{H_{ab}^*(k)}. \quad (76)$$

Inserting these results into the remaining constraints gives a functional equation for H_{ab} ,

$$H_{ab}(l-n-k+m) = H_{ab}^*(k-l) H_{ab}(m-n). \quad (77)$$

We substitute $p = k-l$ and $q = m-n$ and obtain

$$H_{ab}(q-p) = H_{ab}^*(p) H_{ab}(q), \quad (78)$$

entailing

$$\left[\cos \frac{q(a-b)}{2} \cos \frac{p(a-b)}{2} + \sin \frac{q(a-b)}{2} \sin \frac{p(a-b)}{2} \right] \exp \left[-i \frac{(q-p)(a+b)}{2} \right] = \cos \frac{q(a-b)}{2} \cos \frac{p(a-b)}{2} \exp \left[-i \frac{(q-p)(a+b)}{2} \right] \quad (79)$$

from which we get

$$\sin \frac{q(a-b)}{2} \sin \frac{p(a-b)}{2} = 0 \quad (80)$$

for all $p, q \in \mathbb{Z}$. This holds in general by virtue of the quantization condition (60). Hence, we have proven that the mixture assumption (12) for tonal attraction is consistent with the quantum deformation model in an infinite-dimensional Hilbert space. It leads to a particular superposition principle for musical forces (75, 76) that will be investigated in more detail in a subsequent study.

We summarize the results of this subsection. First, we demonstrated that musical tones are represented as Gestalts, i.e. (periodic) wave functions over the circle of fifths which requires the infinite-dimensional Hilbert space of Fourier series. The Schrödinger equation in Fourier space is invariant under continuous $U(1)$ transpositions of a single context tone. For chord contexts, however, this fundamental symmetry is broken, allowing only discrete transpositions from a cyclic group. For Western tonal music, this group is essentially the symmetry of the circle of fifths, i.e. \mathbb{Z}_{12} . Furthermore, we proved that the interaction of tones in chord contexts is not describable through superposition states in Hilbert space. By contrast, musical forces superimpose in Fourier space which leads to a mixing of tonal quantum states by means of discrete convolutions of their pure state kernels.

3.1.5. *Asymmetric deformation*

The mirror symmetry of the spatial deformation model against the tritone $F\sharp$ leads to crucial problems when accounting for the differences between major and minor modes. So far, we considered the conception of static and dynamic attraction only. However, in cognitive music theory some other basic conceptions have been discussed including the idea of graded consonance/dissonance. According to Parncutt (1989), the degree of (musical) consonance of a chord is related to the distribution of potential root tones of a chord. Hereby, the root tone of a chord can be seen as the tone with maximal static attraction given the chord as musical context. In cases with a single, incisive root tone, the chord sounds more consonant than in cases where several root tones compete against each other. Formally, we express the degree of chordal consonance as the static attraction value $p_C(x)$ [Eq. (14)] of the (root) tone with maximum attraction after normalizing the attraction profile (i.e., the attraction values of the 12 tones sum up to 1).

Recently, Johnson-Laird et al. (2012) investigated chords including major triads (CEG), minor triads (CEbG), diminished triads (CEbGb), and augmented triads (CEG#). Table 6 in Sect. 4.1 shows the empirical ratings of the chord’s consonance. Clearly, the major chords exhibit the highest degree of consonance followed by the minor chords. Further, the diminished chords are ranked lower and, at the bottom, we (surprisingly) find the augmented chords. It is not difficult to see that the hierarchic model and the symmetric deformation model predict the same degrees of consonance for major and minor chords.

In order to further improve the predictive power of our quantum deformation model, we consider an asymmetric deformation polynomial of fourth order

$$\gamma(x) = a_0 + a_1(x - \pi) + a_2(x - \pi)^2 + a_3(x - \pi)^3 + a_4(x - \pi)^4, \quad (81)$$

where both, the linear term with coefficient a_1 and the cubic term with coefficient a_3 break the mirror-symmetry against the tritone F#. As above, we demand that the tonic $x = 0 \cong 2\pi$ is not deformed. This leads to two interpolation equations

$$\begin{aligned} \gamma(0) &= 0 \\ \gamma(2\pi) &= 0, \end{aligned}$$

allowing the elimination of two coefficients, e.g. a_3, a_4 :

$$\gamma(x) = a_0 + a_1(x - \pi) + a_2(x - \pi)^2 - \frac{a_1}{\pi^2}(x - \pi)^3 - \frac{a_0 + a_2\pi^2}{\pi^4}(x - \pi)^4. \quad (82)$$

The remaining coefficients receive a straightforward interpretation as intercept: a_0 , skewness: a_1 , and steepness: a_2 (for moderate values). Equation (82) describes the symmetric deformation (24) under the choice $a_0 = \pi/2, a_1 = a_2 = 0$.

We fit both parameters a_1 and a_2 , after inserting (82) with the default values above into the convolution (14), on the C major data set of Krumhansl and Kessler (1982) and obtain $a_1 = -0.14, a_2 = 0.01$ ($r = 0.982$). Finally, we compare our results with those of Johnson-Laird et al. (2012) for C major and C minor triads, and for diminished triads and augmented triads, respectively. The results are presented in section 4.1.2, Tab. 6.

3.2. Dynamic tonal attraction

In this subsection we develop a quantum model based on a deformation of cosine similarity along the circle of fifths for the dynamic tonal attraction experiment of Woolhouse (2009). This model is motivated by Woolhouse' (2009, 2010) interval cycle proximity measure that is described in the next section 3.2.1. Note that dynamic attraction has also successfully been described by Bayesian statistical modeling and Gaussian Markov chains trained on large musical corpora (Temperley 2007, 2008). We further discuss this issue in Sect. 5.

3.2.1. Interval cycle model

In recent research, Woolhouse (2009), Woolhouse and Cross (2010), and Woolhouse (2012) have proposed to explain dynamic tonal attraction in terms of interval cycles. The basic idea is that the dynamic attraction between two pitches is proportional to the number of times the interval spanned by the two pitches must be multiplied by itself to produce some whole number of octaves. Assuming twelve-tone equal temperament, the *interval-cycle proximity (ICP)* of an interval $j \in \mathbb{Z}_{12}$ can be defined as the smallest positive number n such that the product with the interval length (i.e. the number of semitone steps spanned by the interval) is a multiple of twelve (i.e. the maximal interval length). More formally, let $j \in \mathbb{Z}_{12}$ be an interval on the chroma circle. The ICP $n = \text{icp}(j)$ is defined as the smallest integer $n \in \mathbb{N}$, such that

$$nj = 0 \pmod{12} \tag{83}$$

i.e. for a given j one looks for the actually smallest $m \in \mathbb{N}$ such that $nj = 12m$, which eventually gives

$$\text{icp}(j) = \frac{12m}{j} . \tag{84}$$

The following Tab. 3 lists the interval-cycle proximities for all intervals spanned by a given length. For example, one can see that the ICP of the tritone ($j = 6$) is 2 and the ICP of the fifth ($j = 7$) is 12. This has the plausible consequence that, relative to a root tone, the fifth has higher tonal attraction than the tritone.

interval j	0	1	2	3	4	5	6	7	8	9	10	11	12
icp(j)	1	12	6	4	3	12	2	12	3	4	6	12	1

Table 3: Interval cycle proximity (ICP) on chroma circle.

Two particular values of ICP are worth to be mentioned. Relative to the root, the semitone step (the minor second) receives the highest possible $\text{icp}(1) = 12$, while the full-tone step (the major second) assumes its half, $\text{icp}(2) = 6$. This fundamental relation, preferring small intervals in melodic dynamics against larger transitions is substantial for Western music (Curtis and Bharucha 2009, Krumhansl et al. 2000, Narmour 1992, Temperley 2008) and should be maintained in any alternative proposal to the IC model, such as in our quantum model below.

ICP exhibits two interesting symmetries. First, it is obviously invariant under reflection against the tritone $j = 6$, therefore $\text{icp}(j) = \text{icp}(12 - j)$. Second, it is invariant under the transition from the chroma circle to the circle of fifths and vice versa (Woolhouse and Cross 2010): $\text{icp}(j) = \text{icp}(7j \bmod 12)$. As a consequence, ICP assigns the highest value 12 to the minor second ($j = 1$) and to the fourth ($j = 5$). We may thus represent our wave functions alternatively either at the chroma circle, or at the circle of fifths. ICP are plotted along the chroma circle in Fig. 5(b) as the dotted curve.

3.2.2. Deformation model

In order to construct a quantum deformation model of the dynamic tonal attraction data of Woolhouse (2009) we try to interpolate another symmetric fourth-order polynomial

$$\gamma(x) = a_0 + a_2(x - \pi)^2 + a_4(x - \pi)^4 \quad (85)$$

to the transformed and rescaled ICP (cf. Eq. (22))

$$\gamma(x) = \arccos \sqrt{\frac{\text{icp}(x) - 1}{11}}. \quad (86)$$

Equation (86) is ambiguous with respect to the sign of the square root. Taking only the positive square root of ICP into account, involves zeros of

$\gamma(x)$ with multiplicities larger than one, thereby generating a highly fluctuating function which prevents interpolation by a fourth-order polynomial. Thus, we avoid this ambiguity by a smoothing function $\sigma(j)$ tabulated in Tab. 4.

interval j	0	1	2	3	4	5	6	7	8	9	10	11	12
$\sigma(j)$	-1	1	1	1	1	1	-1	1	1	1	1	1	-1

Table 4: Smoothing function σ forcing simple zeros of the ICP deformation.

The smoothing function σ assigns negative values to the unison ($j = 0$), to the tritone ($j = 6$) and to the octave ($j = 12$) and positive values to all other intervals. Consequently, the zeros of $\gamma(x)$ at the minor second ($j = 1$) and the fourth ($j = 5$) become simple zeros, with positive slope for $j = 1$ and negative slope for ($j = 5$), such that the graph of γ traverses the x -axis, thus reducing the complexity of the interpolation. For the values tabulated in Tab. 4, $\gamma(x)$ can be interpolated with a symmetric fourth-order polynomial. Figure 5(a) shows the resulting function $\gamma(x)/\sigma(x)$ in black.

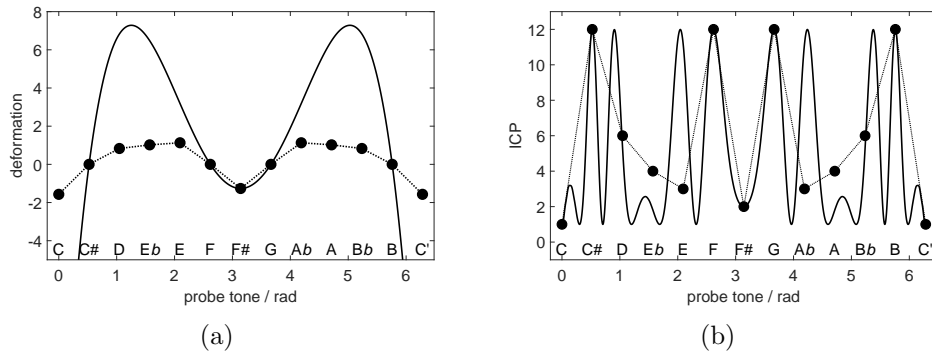


Figure 5: Optimal deformation of the cosine similarity profile for dynamic tonal attraction. (a) Transformed ICP data (86) along the chroma circle (dotted), deformation function (87) (solid). (b) ICP (dotted) and quantum deformation model (solid).

Instead of rigorously modeling the interval cycle model, we use it more as a guideline for our quantum model. Therefore, our model should at least share three important features with ICP: It should prefer small intervals $j = 1, 2$ and it should respect the symmetries of ICP. This choice already

fixes two intervals for our interpolation, namely the zeros of the transformed ICP γ at $j = 1, 5$, where the cosine similarity function (15) should not be deformed at all. For the third interpolation point, we select as in Sect. 3.1.3 the tritone at $j = 6$ as the symmetry center. Then, the three parameters a_0, a_2, a_4 are necessarily (without any fit) obtained from three interpolation equations

$$\begin{aligned}\gamma\left(\frac{\pi}{6}\right) &= 0 \\ \gamma\left(\frac{5\pi}{6}\right) &= 0 \\ \gamma(\pi) &= -\arccos 11^{-\frac{1}{2}}.\end{aligned}$$

The result is the parsimonious parameter-free model

$$\gamma(x) = -\arccos 11^{-\frac{1}{2}} + \frac{936 \arccos 11^{-\frac{1}{2}}}{25\pi^2}(x - \pi)^2 - \frac{1296 \arccos 11^{-\frac{1}{2}}}{25\pi^4}(x - \pi)^4. \quad (87)$$

We plot the original ICP (84) and the quantum probability density (11) of the deformation model (87) Fig. 5(b). Apparently, the kernel resulting from (87) displays some fluctuations over the chroma circle. Interestingly, although the deformation was interpolated only at three intervals $C\sharp$, F and $F\sharp$ in Fig. 5(a), the resulting attraction profile agrees with ICP also at intervals C and D which is crucial for predicting the ratings of unison and major second intervals. However, our interpolation substantially deviates from ICP at minor and major thirds $E\flat$ and E.

Based on the deformation polynomial (87) we also calculate the force densities of dynamic tonal attraction as done for the static case in Eqs. (28 – 30). We evaluate these forces at the chromatic scale degrees over the circle of fifths.

4. Results

This section summarizes the results of our quantum models for tonal attraction which will be compared with traditional models of Lerdahl (1988,

1996), Krumhansl and Kessler (1982) for the static and Woolhouse (2009), Woolhouse and Cross (2010) for the dynamic attraction data.

4.1. Static tonal attraction

First, we consider a symmetric deformation function as derived in Sect. 3.1.4.

4.1.1. Symmetric deformation

Computing the quantum probabilities (11) for the free model gives the results in Fig. 6. Figure 6(a) shows the agreement of the rescaled quantum probability densities with the Krumhansl and Kessler (1982) data for C major, and Fig. 6(b) for C minor. The dotted curves display the results of the Krumhansl and Kessler (1982) experiment, arranged along the circle of fifths. The dashed curves show the continuous quantum probability density $p_C(x)$ [Eq. (14)] obtained from the convolution of the kernel function $p(x)$ (11) of the free pure state wave function $\psi(x)$ [Eq. (3)] over the major triad context CEG (a) and the minor triad context C**E**bG (b). The solid curves display $p_C(x)$ discretely sampled across the circle of fifths.

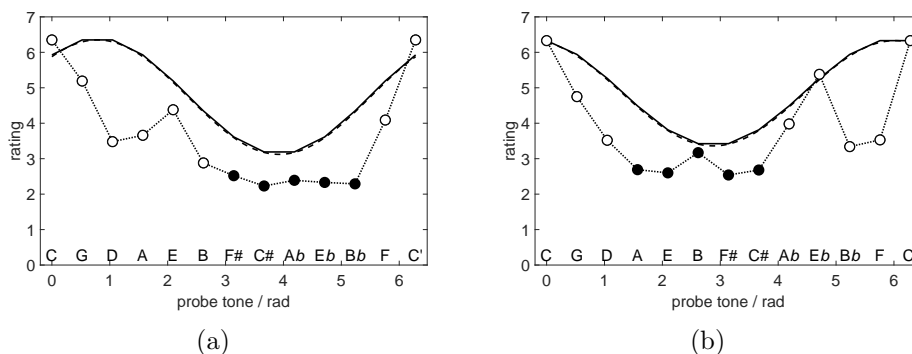


Figure 6: Free quantum (cosine similarity) model for static tonal attraction. Dotted with bullets: rating data $A_{KK}(x)$ of Krumhansl and Kessler (1982) against radian angles at the circle of fifths, dashed: continuous mixed state model $p_C(x)$ [Eq. (14)]. (a) For C major context. (b) For C minor context. Solid: $p_C(x)$ after discrete sampling across the circle of fifths. Open bullets indicate scale (diatonic) tones; closed bullets denote non-scale (chromatic) tones.

In Fig. 7 we present the results of modeling the Krumhansl and Kessler (1982) data (dotted) with the quantum deformation approach [Eqs. (15), (24)]. Computing the mixed state quantum probabilities $p_C(x)$ as convolutions of $p(x)$ [(11)] over the major triad context CEG (a) and the minor triad context CEbG (b) [Eq. (14)] gives the dashed curves. The solid curves display $p_C(x)$ after discrete sampling.

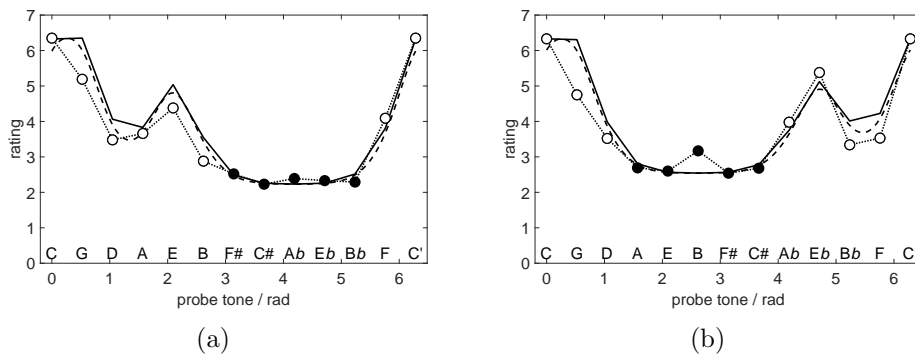


Figure 7: Quantum deformation model for static tonal attraction. Dotted with bullets: rating data $A_{KK}(x)$ of Krumhansl and Kessler (1982) against radian angles at the circle of fifths, dashed: mixed state model $p_C(x)$ [Eq. (14)]. (a) For C major context. (b) For C minor context. Solid: $p_C(x)$ after discrete sampling across the circle of fifths. Open bullets indicate scale (diatonic) tones; closed bullets denote non-scale (chromatic) tones.

Obviously, the mixed state quantum deformation model tracks the experimental data almost perfectly. In particular it is able to unveil the different levels of the hierarchical model: the tonic receives maximal attraction, followed by the fifth, by the third, and eventually by the remaining diatonic scale tones. However, the model does not capture the slight asymmetry between major and minor modes in the data.

Carrying out a correlation analysis between model and data yields the results in Tab. 5.

	hierarchical model	free model		sym. deformation model	
		pure	mixed	pure	mixed
C major	0.98	0.70	0.78	0.89	0.97
C minor	0.95	0.68	0.72	0.80	0.93

Table 5: Correlation coefficients r of four discussed models for static tonal attraction with Krumhansl and Kessler (1982) data. All error probabilities are significantly below 0.05.

The free cosine similarity model already accounts for about $r^2 = 50\%$ of the data’s variance for pure quantum states and slightly improves for mixed quantum states convolved over contextual triads. The deformation model performs much better for pure quantum states and does as good as the hierarchical model based on the generative theory of tonal music. Hence, we conclude that our quantum model is able to explain the experimental results on static tonal attraction using a parameter-free model.

This contrasts with the hierarchical model in methodological and empirical respects. As outlined in Sect. 3.1.1, the hierarchical model stipulates all five levels of description that are essential for predicting tonal attraction ratings. In this sense, the hierarchical model lacks explanatory power. Our deformation model, however, only has to stipulate the triadic level of the hierarchical model. This level is used for calculating the discrete convolution (13) of the deformation kernel (11). From this, the entire major and minor scales are rendered. As discussed in Sect. 3.1.3, the deformation ansatz derives all levels of the hierarchic model, besides the octave level, from the triadic context together with the mixing conjecture and does not require any further stipulation. Thus, our model parsimoniously outperforms the hierarchical model in terms of explanatory power.

Next, we present the musical forces Eqs. (28 – 30) in Fig. 8. Figure 8(a) shows the densities of kinetic energy $T(x)$ [Eq. (25)] (dotted) scaled with 10-fold magnification for better visualization,⁵ magnetic force $F_M(x)$ [Eq. (28)] (dashed), and gravity [Eq. (29)] (solid). Figure 8(b) displays the resultant $F(x)$ [Eq. (30)], all computed for chromatic scale degrees along the circle of fifths.

⁵ There is no corresponding force defined through its gradient.

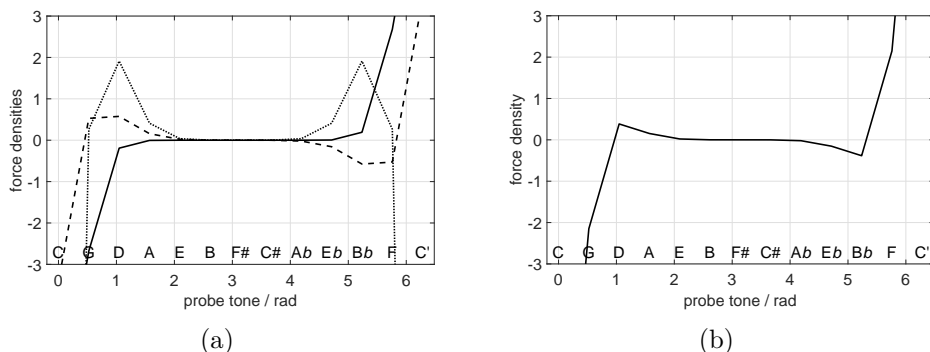


Figure 8: Emergent musical forces of static tonal attraction. (a) Force densities: Dotted: “inertia” $T(x)$, dashed: “magnetism” $F_M(x)$, solid: “gravity” $F_U(x)$. (b) Density of resultant force $F(x)$ [Eq. (30)].

Looking at Fig. 8(a) first, reveals that “gravity” has the largest negative values close to the tonic C on the left and largest positive values close to the tonic C’ one octave higher, on the right of the circle of fifths. As negative force pulls toward smaller x -values while positive force pulls toward larger x -values, this indicates that the tonic C attracts the fifth G. Since “gravity” is monotonically increasing, it also shows that G attracts D, D attracts A, and so forth with decreasing magnitude for increasing distance from the tonic. Beyond the tritone F# \sharp , F is attracted by C’, Bb by F, and Eb by Bb and so forth. Interestingly, the tritone is an unstable equilibrium, as $F_G(\pi) = 0$ with positive slope. For “magnetism” things are a bit more complicated. $F_M = 0$ at tones F# \sharp but also between C and G as well as between F and C’. This makes the tritone a stable equilibrium, but G and F unstable equilibria, i.e. saddles, with respect to “magnetism”. The tonic therefore “magnetically” attracts G and F, whereas all tones between G and F are “magnetically” attracted by F# \sharp , making the tritone F# \sharp a “magnetic trap” in this region. Inertia, eventually, assumes its maxima at the supertonic D and at Bb, which does not belong to the scale of C major. Both therefore have to be regarded as transient tones with maximal instability.

Perhaps even more instructive is Fig. 8(b) depicting the resultant force density $F(x)$. Here again, the tonic appears as a center of force. Zeros of $F(x)$ are equilibrium points which are either unstable for positive slope or stable for negative slope. On the one hand, there are two unstable equilibria

around $x = 0.8$ (supertonic D) and $x = 5.4$ (B♭). On the other hand, the only equilibrium at $x = \pi$ is stable, which is precisely the tritone. Because the resultant force is low in this region, tones are trapped by the tritone F♯.

4.1.2. Asymmetric deformation

Finally, we present the results for the asymmetric deformation model from Sect. 3.1.5 in Tab. 6. The asymmetric quantum model is able to explain the correct consonance ranking of major (CEG), minor (CE♭G), diminished (CE♭G♭), and augmented triads (CEG♯), respectively (Johnson-Laird et al. 2012). For the hierarchical model the correlation is $r = 0.93$ ($p = 0.07$), for the asymmetric deformation model we have $r = 0.95$ ($p = 0.05$).

	emp. consonance	hier. model	asym. deformation model
major	5.33	0.49	0.54
minor	4.59	0.49	0.52
diminished	3.11	0.34	0.36
augmented	1.74	0.33	0.34

Table 6: Empirical consonance ratings and model predictions for common triads. The predictions of the models concern the strength of strongest static attraction using normalized attraction profiles.

Summarizing, we consider a case of symmetry breaking in cognitive musicology, breaking the mirror symmetry of the tonal attraction kernel in analogy to Parncutt (2011). In this way, we overcome some weaknesses of the classical attraction model based on tonal hierarchies, which cannot account for the differences between major and minor modes. Consequently, we get a suitable model not only for static attraction profiles but also for graded consonance/dissonance. The ability for unification — grasping different phenomena in a systematic way — is one of the trademarks of quantum theory, which is correspondingly apparent in the domain of quantum cognition as well.

4.2. Dynamic tonal attraction

Here, we present the results of modeling the Woolhouse (2009) data with the quantum deformation model that was somewhat motivated by the interval cycle model. Computing the probability densities (11) for five contexts gives the results in Fig. 9. Figure 9(a) shows the agreement of the model with the Woolhouse (2009) data for C major, (b) for C minor, (c) for the dominant seventh, (d) for French sixth, and (e) for half-diminished seventh. The dotted curves present the original results of the Woolhouse (2009) experiment. The dashed curves display the continuous quantum probability density p_C obtained from the mixture of pure states over all context tones in the respective chords: major triad CEG (a), minor triad CE \flat G (b), dominant seventh CEG \flat B \flat (c), French sixth CEG \flat B \flat (d), and half-diminished seventh CE \flat G \flat B \flat (e).

Finally, we also deliver our model’s prediction (f) for the famous “Tristan chord” from Richard Wagner’s opera *Tristan und Isolde* (1860). Following Woolhouse (2012), the tension induced by the “Tristan chord” E \flat FG \sharp B, which is further strengthened by an intervening French sixth E \flat FAB, betokened by a single A, is eventually resolved by the chord EG \sharp DB \flat .⁶

⁶ At the moment, no empirical data are available for the “Tristan chord”.

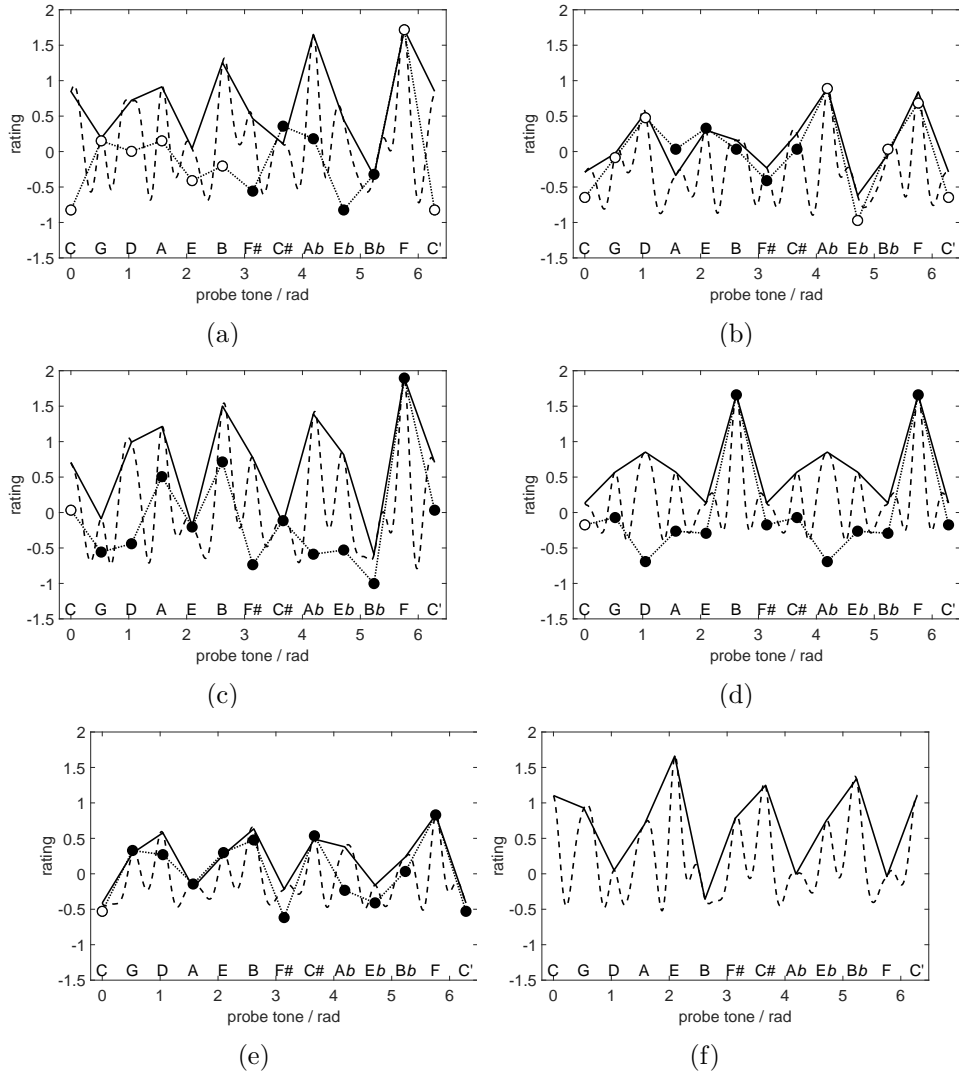


Figure 9: Quantum deformation model for dynamic tonal attraction data. Dotted with bullets: Rating data $A_W(x)$ of Woolhouse (2009) against radian angles at the circle of fifths. Dashed: quantum probability density $p_C(x)$ of the mixed state model (14). (a) For C major context. (b) For C minor context. (c) For dominant seventh. (d) For French sixth. (e) For half-diminished seventh. (f) For “Tristan chord”. Solid: mixed state density after sampling along the circle of fifths.

The mixed state quantum deformation model makes the correct predictions F, A and C for the C major context interpreted as the dominant of F

major, and G, B, and D interpreted as the subdominant of G major [Fig. 9(a)]. However, the agreement with model and data is confined to F, G, B, and C \sharp . For C minor shown in [Fig. 9(b)], the model almost perfectly agrees with the experimental results: highest attraction values are assigned to A \flat , F, and D. The model conforms also with music-theoretic predictions, resolving either the dominant of F minor into its tonic FA \flat C, or the subdominant of G minor into GB \flat D. Also for the dominant seventh [Fig. 9(c)] the model correctly predicts F as the most likely resolution. For E and C \sharp model and data agree quite well. The French sixth context [Fig. 9(d)] correctly predicts resolution at B and F, but there is not much correlation with other data points. This is different for the half-diminished seventh plotted in [Fig. 9(e)], where the model curve tracks the experimental data quite well, besides A \flat . Figure 9(f) demonstrates a remarkable performance of our model predicting the resolution of the “Tristan chord”. The predicted attraction rate is maximal at E and B \flat , those tones that belong to the resolving chord EG \sharp DB \flat . Interestingly, a similar analysis (not shown) for the intervening French sixth also yields large attraction values for E and B \flat , which are thereby further enhanced. In addition, the French sixth also increases attraction rates for the resolving G \sharp and D.

The quality of our model is assessed by the regression analysis presented in Tab. 7.

	IC model	deformation model
C major	0.69	0.44
C minor	0.76	0.93
dominant seventh	0.76	0.65
French sixth	0.79	0.76
half-diminished seventh	0.89	0.90

Table 7: Correlation coefficients r of two discussed models for dynamic tonal attraction with Woolhouse (2009) data. All error probabilities are significantly below 0.05.

The correlation coefficients confirm the outcome of visually inspecting Fig. 9. For C minor and the half-diminished seventh our quantum model performs slightly better than the IC model of Woolhouse (2009) and Woolhouse and Cross (2010). Moreover, our model correctly predicts the resolution of the “Tristan chord” (Woolhouse 2012). However, the main advantage of the quantum

deformation model goes beyond the Woolhouse model and is able describing both the static and the dynamic attraction data.

Next we present the musical forces (28 – 30) in Fig. 10. Since the forces depend up to the third derivative of the deformation γ , it is not possible to show them on the continuum of the circle of fifths. Hence the results presented below may be taken with some caution.

Figure 10(a) shows the densities of kinetic energy $T(x)$ [Eq. (25)] (dotted), magnetic force $F_M(x)$ [Eq. (28)] (dashed), and gravity [Eq. (29)] (solid). As gravity is absolutely predominating, we rescale inertia and magnetism by a factor of 30 here. Figure 10(b) displays the resultant $F(x)$ [Eq. (30)], all computed for chromatic scale degrees along the circle of fifths.

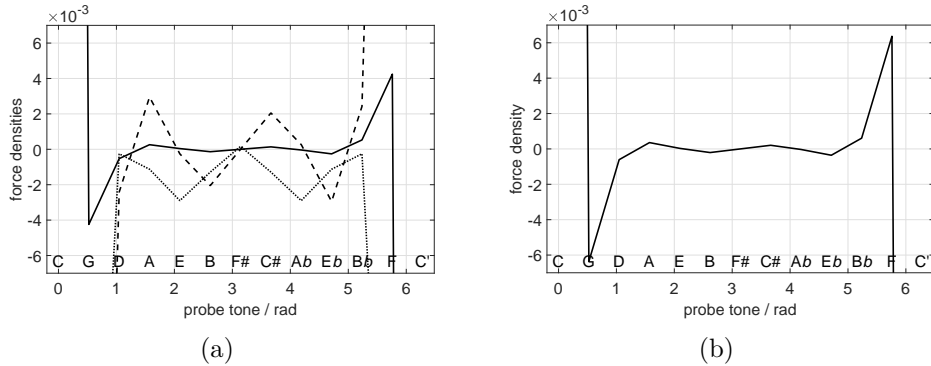


Figure 10: Emergent musical forces of dynamic tonal attraction. (a) Force densities: Dotted: “inertia” $T(x)$, dashed: “magnetism” $F_M(x)$, solid: “gravity” $F_U(x)$. (b) Density of resultant force $F(x)$ [Eq. (30)].

Figure 10(a) reveals that “gravity” starts with large positive values at the tonic C and reaches large negative values at the octave C’. Hence, C is attracted by G and C’ by F. Moreover, “gravity” exhibits seven zeros: close to G, between D and A, between E and B, at the tritone F#, between C# and Ab, between Eb and Bb, and close to F. The first, around G has negative slope and is hence a stable attractor, the second between D and A has positive slope, making it unstable, the third is stable, again, the tritone becomes unstable, the fifth stable, the sixth unstable and the last around F is stable. Therefore, D is attracted by G, A by E, Eb by Ab and Bb by

F. However, around the tritone $F\sharp$, “gravity” almost vanishes. A similar behavior is shown by “magnetism”, which displays five equilibria points with different stabilities. Finally, “inertia” is mainly negative, thus preferring descending motion along the chromatic scale.

Because “gravity” overcomes all other dynamical forces, Fig. 10(b), showing the resultant force density $F(x)$, presents almost the same picture with seven equilibrium points: A stable attractor at G, an unstable between D and A, another stable one between E and B, the tritone being unstable, a stable attractor between $C\sharp$ and $A\flat$, an unstable between $E\flat$ and $B\flat$, and finally, F being stable. Moreover, our model also correctly predicts small interval steps in comparison to larger steps, as musical force is relatively large for C and (as well as F and C’ on the opposite side of the octave). For the range D to $B\flat$, the dynamic force becomes negligible.

5. Discussion

Tonal attraction is an important issue in the psychology of music. In this study, we have discussed two kinds of tonal attraction as investigated by probe tone experiments. Static tonal attraction refers to the stability or instability of tones or chords in a certain context, establishing a tonal key. By contrast, dynamic tonal attraction reflects the predictability of tones or chords continuing a preestablished melodic or harmonic context (Temperley 2008). In the paradigm of probe tone experiments (Krumhansl and Shepard 1979, Krumhansl 1979), static and dynamic attraction are investigated by means of different kinds of instructions: On the one hand, in a static attraction experiment, subjects are asked to rate how well a presented probe tone fits to a priming context (Krumhansl and Kessler 1982). In a dynamic attraction experiment, on the other hand, subjects are asked to rate how well a given probe tone completes or resolves the priming context, both melodically or harmonically (Woolhouse 2009).

It was the aim of this study to integrate structural and probabilistic theories of computational music theory into a unified framework. On the one hand, structural accounts such as the generative theory of tonal music are guided by principle musicological insights about the intrinsic symmetries of

Western tonal music (Lerdahl and Jackendoff 1983, Lerdahl 1988, 1996). On the other hand, probabilistic accounts such as Bayesian models or Gaussian Markov chains are able to describe melodic progression through statistical correlations in large music corpora (Bod 2002, Temperley 2007, 2008). Here, we argued that quantum approaches to music cognition are able to unify symmetry and (quantum) probability in a single framework for data from static and dynamic attraction experiments.

In a first attempt to describing the static attraction data of Krumhansl and Kessler (1982), we realized that simply rearranging the data points according to the important circle of fifths, instead of increasing physical pitch frequency, revealed a systematic pattern of periodic attraction: tones close to the tonic are more attractive than tones in the vicinity of the tritone. Since this periodicity could be expressed as a cosine similarity measure, often used in quantum cognition models of similarity judgements (Pothos et al. 2013, Pothos and Trueblood 2015), we were led to the formulation of a quantum model of tonal attraction by means of a “wave function” defined over the circle group as “configuration space” which includes the circle of fifths as a subgroup. We referred to this model as to the “free” model because its wave function obeys a “free particle” Schrödinger equation without any force terms contributing to its Hamiltonian.

Important insights from our free quantum model are: First, its Hilbert space is essentially two-dimensional which proves its equivalence with an earlier qubit model proposed by Blutner (2015). Second, musical transpositions, i.e. translations along the circle of fifths as mediated by the generator of its cyclic group, are represented, just in the sense of harmonic analysis, through unitary transformations in Hilbert space.

In order to improve our free model, we developed a “deformation” quantum model, still based on cosine quantum similarity, but introducing a deformation of interval lengths over the circle of fifths. We described this deformation function as a symmetric polynomial of fourth order, and determined its parameters from two necessary interpolation conditions, saying that the tonic should not be deformed at all, while the tritone receives maximal deformation. The resulting “wave function” is also governed by a Schrödinger equation whose Hamiltonian consists of three additive terms that could be identified as “inertia”, “magnetism” and “gravity”, the very

same forces (Larson and van Handel 2005, Larson 2012) that are metaphorically used in the hierarchical model of static tonal attraction (Lerdahl 1988, 1996, Krumhansl and Kessler 1982, Krumhansl and Cuddy 2010).

For the tonic context, we calculated the musical force densities over the circle of fifths and confirmed the tonic as a “center of gravity” attracting all other tones in its vicinity. However, in contrast to predictions of the hierarchical model, we also established the tritone as a “magnetic trap”, attracting its neighborhood with increasing pull for increasing distance. This finding is apparently at variance with the conventional interpretation of musical magnetism which states that magnetic force increases for decreasing distance (Larson and van Handel 2005, Larson 2012).

Our prediction of the tritone as a “magnetic trap” calls for further experimental investigation. We therefore suggest to designing probe tone experiments where this possibility could be further explored.

In order to assess the tonal attraction for complex priming stimuli such as chords or cadences, we followed a suggestion recently conjectured by Woolhouse and Cross (2010) and exploited by Blutner (2015) to compute the discrete convolution of a kernel function, the quantum probability obtained from the squared wave function, and a uniform distribution over all context tones. As contexts, we assumed the tonic triads of the C major and C minor keys for static attraction, here. This is similar to the hierarchical model of Lerdahl (1988, 1996), where the tonic triad comprises level C in the hierarchy. As a result, our model precisely reproduced the experimental data with comparable statistical performance as the hierarchical model. However, while the hierarchical model has to stipulate the existence of all five levels in the hierarchy, our model only refers to the C level. The other levels A – E required by the hierarchical model are deduced from our model. Therefore, our quantum model parsimoniously outperforms the hierarchical model of static attraction with respect to explanatory power.

Applying harmonic analysis to the quantum deformation model, we derived quantization conditions for musical wave functions in infinite-dimensional Fourier space. Combining musical transposition symmetry with the discrete convolution model for chordal contexts, we derived the emergence of the chromatic 12-tone cyclic group through symmetry breaking. Other possible sym-

metries are cyclic groups considered in microtonality approaches (Balzano 1980).

However, the symmetric deformation model for static tonal attraction does not correctly describe the observed asymmetry between major and minor modes in the Krumhansl and Kessler (1982) data. This is also a problem for the hierarchical model as well. We therefore additionally presented an asymmetric deformation model that breaks the mirror symmetry against the tritone. Fitting two free parameters of this model to the major context, we were able to achieve substantial improvement also for minor keys and an understanding for the different degrees of consonance for major, minor, diminished, and augmented chords.

For dynamic tonal attraction we devised a similar quantum model based on a fourth-order polynomial deformation. This construction was guided by the interval cycle model of Woolhouse and Cross (2010) and Woolhouse (2009) and in agreement to related models that prefer small intervals over longer ones for melodic and harmonic dynamics (Curtis and Bharucha 2009, Krumhansl et al. 2000, Narmour 1992, Temperley 2008).

Concerning dynamic attraction, we took the ICP model as a guideline for constructing a quantum deformation model of dynamic attraction. The preference of the ICP model for small interval steps should be met by our model. Furthermore, we claimed that the symmetries of the ICP model should be preserved. This led us to another kernel function over the circle of fifths that deviated from ICP at minor and major third intervals. Our model performed comparably well as the ICP model in a regression analysis. Interestingly, our model confirms predictions about the resolution of context chords based on musical harmony theory with good accuracy.

Computing dynamic musical forces for the tonic context, our model predicts essentially ascending or descending melodic lines, preferring small interval steps. Also this result calls for experimental investigation, using music from other cultures, e.g. Indian or Chinese, as stimuli in corresponding probe tone experiments (Curtis and Bharucha 2009, Krumhansl et al. 2000).

Sofar, we have constructed both quantum models of tonal attraction as wave functions solving stationary Schrödinger equations. However, dy-

namics always refers to the time-dependent Schrödinger equation in quantum physics. Thus, it is desirable to solve the dynamic attraction problem with the time-dependent Schrödinger equation but using the Hamiltonian for the static attraction case. Such a grand unification of musical quantum cognition will also conform with Bayesian and Markovian models of music cognition (Temperley 2007, 2008), because Markov chains describe the dynamics of stochastic processes. Moreover, there are important formal similarities between Chapman-Kolmogorov and Fokker-Planck equations in stochastic dynamics and the Schrödinger equation or unitary evolution in quantum dynamics (Busemeyer and Bruza 2012).

Finally, we address the possible relevance of our work to the cognitive neuroscience of music perception. The behavioral findings of Krumhansl and Kessler (1982) and Woolhouse (2009) have been supported by neuropsychological experiments in the event-related brain potential (ERP) (Granot and Hai 2009, Limb 2006) and in the functional magnetic resonance (fMRI) paradigms (Durrant et al. 2007, Janata et al. 2002, Koelsch et al. 2002, Limb 2006, Vaquero et al. 2016). The first three fMRI studies used melodies with harmonic modulation from one key into another key as stimuli and reported significant anatomical differences for key changes. In particular, Janata et al. (2002), who carried out a regression analysis of fMRI data with self-organized maps trained upon the third torus as tonal space (Janata et al. 2002, Purwins et al. 2007), made the strong claim that the rostromedial prefrontal cortex exhibits a neural tonotopic representation of the third torus.

From a computational point of view, our quantum models describe tonal attraction through “wave functions” obeying the stationary Schrödinger equation. In the most general setting, similar differential equations are also often employed in the disciplines of neural field (Coombes et al. 2014a) and dynamic neural field theory (Lins and Schöner 2014, beim Graben and Potthast 2014) within computational neuroscience, where they appear as so-called brain wave equations (Nunez 1974, Coombes et al. 2014a). In dynamic neural field theory, fields are regarded as functions over *abstract feature spaces* and we might consider the circle of fifths in our approach as such a feature space. These neural fields are clearly real-valued functions in contrast to the generically complex wave functions solving the Schrödinger equation. However, according to Bohm (1952), the Schrödinger equation for one complex field is equivalent to two coupled real fields describing the motion of a classical

particle in a “quantum mechanical potential” and its respective field dynamics (cf. Filk (2016) for a related proposal in computational neuroscience). In quantum theory this leads to disputably nonlocal representations. Yet in neural field theory, nonlocal interactions are ubiquitous due to long-range synaptic connectivity. Thus, quantum models of tonal attraction may find their neurophysiological counterparts in the organization of cortical areas (Sengupta et al. 2016, Wright et al. 2006).

6. Conclusions

This study applies methods from the quantum cognition framework to tonal attraction. In probe tone experiments, music psychologists measure the likelihood of chromatic probe tones relative to a priming context. Depending on the particular instruction, the subject’s ratings assess either the degree of fit between a probe tone and a key context (static attraction), or the degree of predictability of a probe tone given a preceding context (dynamic attraction). A first attempt reveals that tonal attraction correlates with quantum similarity between tones across the important circle of fifths. Deforming the distances between tones leads to two quantum wave functions, one for static attraction, the second for dynamic attraction, solving a stationary Schrödinger equation with a Hamiltonian that comprises three musical forces: inertia, magnetism and gravity. We compute these forces for tonic contexts and compare them with predictions of the hierarchical model in the static case and of the interval cycle model for the dynamic case. Instead of metaphorical interpretations, our parsimonious quantum models provide precise and rigorous results with greater explanatory power.

Appendix

Geometric illustration of static deformation

In this appendix, we construct the geometric representation of the symmetric quantum deformation model from section 3.1.3 that is illustrated in Fig. 1(b) in the Introduction Sect. 1. This construction rests on another important physical symmetry, the invariance of the line element of space-time

in Einstein's general theory of relativity. Since we only consider stationary states in this study, we focus on the line element ds in differential geometry here.

Consider the unit circle parameterized by the phase angle $\phi : [0, 2\pi[\rightarrow [0, 2\pi[$, with $\phi(t) = t$ as the angle between the tonic C at the y -axis and a probe tone at the periphery of the unit circle, indicated in Fig. 1(b). In Cartesian coordinates we have

$$\begin{aligned} x(t) &= \sin \phi(t) = \sin t \\ y(t) &= \cos \phi(t) = \cos t . \end{aligned} \tag{88}$$

A general closed contour Γ is then described as

$$\begin{aligned} x(t) &= r(t) \sin \phi(t) \\ y(t) &= r(t) \cos \phi(t) . \end{aligned} \tag{89}$$

For static attraction deformation we set

$$\phi(t) = 2\gamma(t) \tag{90}$$

with (24) above. Note that $\gamma : [0, 2\pi[\rightarrow [0, \pi/2[$. We now seek a radius function $r(t)$ that compensates the decreasing distances between tones approaching the tritone $F\sharp$. This is achieved by the invariance of the infinitesimal line element ds .

The line element is defined as

$$ds^2 = dx^2 + dy^2 . \tag{91}$$

For the unit circle (89), we immediately obtain

$$ds^2 = dt^2 , \tag{92}$$

whereas the deformation (89) and (90) leads to

$$ds^2 = \left[\left(\frac{dr(t)}{dt} \right)^2 + 4r(t)^2 \left(\frac{d\gamma(t)}{dt} \right)^2 \right] dt^2 , \tag{93}$$

such that invariance of the line element entails

$$\left(\frac{dr(t)}{dt}\right)^2 + 4r(t)^2 \left(\frac{d\gamma(t)}{dt}\right)^2 = 1. \quad (94)$$

Equation (94) is a nonlinear differential equation for the desired radius of the deformation. We solve Eq. (94) numerically and find the deformation illustrated in Fig. 1(a).

Derivation of the magnetic force term

According to quantum mechanical gauge theory, the impact of a magnetic field, described by a (one-dimensional) vector potential $A(x)$ at site x , is obtained from the free particle Schrödinger equation $T\psi(x) = E\psi(x)$ with Hamiltonian $H = T = p^2$ and momentum operator $p = -i\partial/\partial x$ through *minimal coupling* by the substitution $p \rightarrow p - A$.⁷ Inserting this into T gives the gauged Schrödinger equation

$$(p - A(x))^2\psi(x) = E\psi(x).$$

Expanding the bracket yields

$$\begin{aligned} (p - A(x))(p - A(x))\psi(x) &= E\psi(x) \\ (p^2 - pA(x) - A(x)p + A(x)^2)\psi(x) &= E\psi(x) \\ T\psi(x) - A(x)p\psi(x) + A(x)^2\psi(x) &= E\psi(x) \\ -\psi''(x) + iA(x)\psi'(x) + A(x)^2\psi(x) &= E\psi(x), \end{aligned}$$

where we have utilized Coulomb gauge $pA(x) = -iA'(x) = 0$ in line two.

This justifies to identify the coefficient of the first derivative of the wave function in the deformation model (16) with musical magnetic force.

⁷ Note that we normalize particularly physical quantities such as mass m , charge q , light speed c and Planck's quantum of action \hbar to natural units = 1 here. We also reduce our discussion to a simplified one-dimensional picture.

Acknowledgments

We thank Maria Mannone, Serafim Rodrigues and Günther Wirsching for valuable comments on an earlier version of the manuscript.

References

References

- Aerts, D. (2009). Quantum structure in cognition. *Journal of Mathematical Psychology*, 53(5):314 – 348.
- Araya-Salas, M. (2012). Is birdsong music? *Significance*, pages 4 – 7.
- Balzano, G. J. (1980). The group-theoretic description of 12-fold and micro-tonal pitch systems. *Computer Music Journal*, 4(4):66 – 84.
- beim Graben, P. (2014). Order effects in dynamic semantics. *Topics in Cognitive Science*, 6(1):67 – 73.
- beim Graben, P. and Atmanspacher, H. (2009). Extending the philosophical significance of the idea of complementarity. In Atmanspacher, H. and Primas, H., editors, *Recasting Reality. Wolfgang Pauli's Philosophical Ideas and Contemporary Science*, pages 99 – 113. Springer, Berlin.
- beim Graben, P. and Blutner, R. (2017). Toward a gauge theory of musical forces. In de Barros, J. A., Coecke, B., and Pothos, E., editors, *Quantum Interaction. 10th International Conference (QI 2016)*, volume 10106 of *LNCS*, pages 99 – 111. Springer, Cham.
- beim Graben, P. and Potthast, R. (2014). Universal neural field computation. In Coombes et al. (2014b), pages 299 – 318.
- Blutner, R. (2012). Questions and answers in an orthoalgebraic approach. *Journal of Logic, Language and Information*, 21(3):237 – 277.
- Blutner, R. (2015). Modelling tonal attraction: tonal hierarchies, interval cycles, and quantum probabilities. *Soft Computing*, pages 1 – 19.

- Blutner, R. and beim Graben, P. (2013). The (virtual) conceptual necessity of quantum probabilities in cognitive psychology. *Behavioral and Brain Sciences*, 36(3):280 – 281.
- Blutner, R. and beim Graben, P. (2016). Quantum cognition and bounded rationality. *Synthese*, 193:3239 – 3291.
- Bod, R. (2002). Memory-based models of melodic analysis: Challenging the Gestalt principles. *Journal of New Music Research*, 31(1):27 – 36.
- Bohm, D. (1952). A suggested interpretation of the quantum theory in terms of “hidden” variables. I. *Physical Reviews*, 85:166 – 179.
- Bohr, N. (1950). On the notions of causality and complementarity. *Science*, 111(2873):51 – 54.
- Busemeyer, J. R. and Bruza, P. D., editors (2012). *Quantum Models of Cognition and Decision*. Cambridge University Press.
- Chiara, M. L. D., Giuntini, R., Leporini, R., Negri, E., and Sergioli, G. (2015). Quantum information, cognition and music. *Frontiers in Psychology*, 6(1583).
- Coombes, S., beim Graben, P., and Potthast (2014a). Tutorial on neural field theory. In Coombes et al. (2014b), pages 1 – 43.
- Coombes, S., beim Graben, P., Potthast, R., and Wright, J., editors (2014b). *Neural Fields: Theory and Applications*. Springer, Berlin.
- Curtis, M. E. and Bharucha, J. J. (2009). Memory and musical expectation for tones in cultural context. *Music Perception: An Interdisciplinary Journal*, 26(4):365 – 375.
- Durrant, S., Miranda, E. R., Hardoon, D., Shawe-Taylor, J., Brechmann, A., and Scheich, H. (2007). Neural correlates of tonality in music. In *Proceedings of the NIPS Conference Workshop on Music, Brain & Cognition*.
- Filk, T. (2016). Non-classical probabilities in pilot wave models and neural networks. *Journal of Mathematical Psychology*, 74(Supplement C):92 – 98.
- Fraser, J. (1908). A new visual illusion of direction. *British Journal of Psychology*, 2(3):307.

- Granot, R. Y. and Hai, A. (2009). Electrophysiological evidence for a two-stage process underlying single chord priming. *NeuroReport*, 20(9).
- Haag, R. (1992). *Local Quantum Physics: Fields, Particles, Algebras*. Springer, Berlin.
- Janata, P. (2007). Navigating tonal space. In Selfridge-Field, E. and Hewlett, W. B., editors, *Tonal Theory for the Digital Age*, volume 15 of *Computing in Musicology*, pages 39 – 50. MIT Press, Cambridge (MA).
- Janata, P., Birk, J. L., Horn, J. D. V., Leman, M., Tillmann, B., and Bharucha, J. J. (2002). The cortical topography of tonal structures underlying western music. *Science*, 298(5601):2167 – 2170.
- Johnson-Laird, P. N., Kang, O. E., and Leong, Y. C. (2012). On musical dissonance. *Music Perception: An Interdisciplinary Journal*, 30(1):19 – 35.
- Khrennikov, A. Y. (2010). *Ubiquitous Quantum Structure: From Psychology to Finance*. Springer, Berlin.
- Koelsch, S., Gunter, T. C., von Cramon, D. Y., Zysset, S., Lohmann, G., and Friederici, A. D. (2002). Bach speaks: a cortical “language-network” serves the processing of music. *NeuroImage*, 17(2):956 – 966.
- Köhler, W. (1969). *The Task of Gestalt Psychology*. Princeton University Press, New Jersey.
- Krumhansl, C. L. (1979). The psychological representation of musical pitch in a tonal context. *Cognitive Psychology*, 11(3):346 – 374.
- Krumhansl, C. L. and Cuddy, L. L. (2010). A theory of tonal hierarchies in music. In Jones, M. R., Fay, R. R., and Popper, A. N., editors, *Music Perception*, Springer Handbook of Auditory Research, pages 51 – 87. Springer, New York.
- Krumhansl, C. L. and Kessler, E. J. (1982). Tracing the dynamic changes in perceived tonal organization in a spatial representation of musical keys. *Psychological Review*, 89(4):334 – 368.

- Krumhansl, C. L. and Shepard, R. N. (1979). Quantification of the hierarchy of tonal functions within a diatonic context. *Journal of Experimental Psychology: Human Perception and Performance*, 5(4):579.
- Krumhansl, C. L., Toivanen, P., Eerola, T., Toiviainen, P., Järvinen, T., and Louhivuori, J. (2000). Cross-cultural music cognition: Cognitive methodology applied to North Sami yoiks. *Cognition*, 76(1):13 – 58.
- Lakoff, G. and Johnson, M. (1980). *Metaphors We Live By*. University of Chicago Press, Chicago.
- Lambert-Mogiliansky, A. and Dubois, F. (2016). Our (represented) world: A quantum-like object. In Dzhafarov, E., Jordan, S., Zhang, R., and Cervantes, V., editors, *Contextuality from Quantum Physics to Psychology*, volume 6 of *Advanced Series on Mathematical Psychology*, World Scientific.
- Larson, S. (2012). *Musical Forces: Motion, Metaphor, and Meaning in Music*. Indiana University Press.
- Larson, S. and van Handel, L. (2005). Measuring musical forces. *Music Perception: An Interdisciplinary Journal*, 23(2):119 – 136.
- Lerdahl, F. (1988). Tonal pitch space. *Music Perception: An Interdisciplinary Journal*, 5:315 – 350.
- Lerdahl, F. (1996). Calculating tonal tension. *Music Perception: An Interdisciplinary Journal*, 13(3):319 – 363.
- Lerdahl, F. (2015). Concepts and representations of musical hierarchies. *Music Perception: An Interdisciplinary Journal*, 33(1):83 – 95.
- Lerdahl, F. and Jackendoff, R. (1983). *A Generative Theory of Tonal Music*. MIT Press, Cambridge (MA).
- Limb, C. J. (2006). Structural and functional neural correlates of music perception. *The Anatomical Record Part A: Discoveries in Molecular, Cellular, and Evolutionary Biology*, 288A(4):435 – 446.
- Lins, J. and Schöner, G. (2014). A neural approach to cognition based on dynamic field theory. In Coombes, S., beim Graben, P., Potthast, R., and Wright, J., editors, *Neural Fields: Theory and Applications*, pages 319 – 339. Springer, Berlin.

- Mannone, M. (2018). Knots, music, and DNA. *Journal of Creative Music Systems*, 2(2).
- Mannone, M. and Compagno, G. (2013). Characterization of the degree of musical non-Markovianity. arXiv:1306.0229 [physics.data-an].
- Mannone, M. and Mazzola, G. (2015). Hypergestures in complex time: Creative performance between symbolic and physical reality. In Collins, T., Meredith, D., and Volk, A., editors, *Proceedings of the 5th International Conference on Mathematics and Computation in Music (MCM 2015)*, pages 137 – 148, Cham. Springer.
- Mazzola, G. (1990). *Geometrie der Töne*. Birkhäuser, Basel.
- Mazzola, G. (2002). *The Topos of Music: Geometric Logic of Concepts, Theory, and Performance*. Birkhäuser, Basel.
- Mazzola, G., Mannone, M., and Pang, Y. (2016). *Cool Math for Hot Music*. Computational Music Science. Springer, Cham.
- Milne, A. J., Laney, R., and Sharp, D. B. (2015). A spectral pitch class model of the probe tone data and scalic tonality. *Music Perception: An Interdisciplinary Journal*, 32(4):364 – 393.
- Milne, A. J., Sethares, W. A., Laney, R., and Sharp, D. B. (2011). Modelling the similarity of pitch collections with expectation tensors. *Journal of Mathematics and Music*, 5(1):1 – 20.
- Narmour, E. (1992). *The Analysis and Cognition of Melodic Complexity: The Implication-Realization Model*. University of Chicago Press, Chicago (IL).
- Nunez, P. L. (1974). The brain wave equation: A model for the EEG. *Mathematical Biosciences*, 21(3-4):279 – 297.
- Parncutt, R. (1989). *Harmony: A Psychoacoustical Approach*. Springer, Berlin.
- Parncutt, R. (2011). The tonic as triad: Key profiles as pitch salience profiles of tonic triads. *Music Perception: An Interdisciplinary Journal*, 28(4):333 – 366.

- Pauli, W. (1950). Die philosophische Bedeutung der Komplementarität. *Experimentia*, 6:72 – 81.
- Pothos, E. M. and Busemeyer, J. R. (2013). Can quantum probability provide a new direction for cognitive modeling? *Behavioral and Brain Sciences*, 36:255 – 274.
- Pothos, E. M., Busemeyer, J. R., and Trueblood, J. S. (2013). A quantum geometric model of similarity. *Psychological Review*, 120(3):679 – 696.
- Pothos, E. M. and Trueblood, J. S. (2015). Structured representations in a quantum probability model of similarity. *Journal of Mathematical Psychology*, 64-65:35 – 43.
- Purwins, H., Blankertz, B., and Obermayer, K. (2007). Toroidal models in tonal theory and pitch-class analysis. In Selfridge-Field, E. and Hewlett, W. B., editors, *Tonal Theory for the Digital Age*, volume 15 of *Computing in Musicology*, pages 73 – 98. MIT Press, Cambridge (MA).
- Schönberg, A. (1978). *Theory of Harmony*. University of California Press, Berkeley (CA).
- Schrödinger, E. (1926). Quantisierung als Eigenwertproblem – Erste Mitteilung. *Annalen der Physik*, 79:361 – 376.
- Sengupta, B., Tozzi, A., Cooray, G. K., Douglas, P. K., and Friston, K. J. (2016). Towards a neuronal gauge theory. *PLoS Biology*, 14(3):1 – 12.
- Stolzenburg, F. (2015). Harmony perception by periodicity detection. *Journal of Mathematics and Music*, 9(3):215 – 238.
- Temperley, D. (2007). *Music and Probability*. MIT Press, Cambridge (MA).
- Temperley, D. (2008). A probabilistic model of melody perception. *Cognitive Science*, 32(2):418 – 444.
- v. Helmholtz, H. (1877). *On the Sensations of Tones*. Dover, New York (NY). Translated by A. J. Ellis.
- Vaquero, L., Hartmann, K., Ripollés, P., Rojo, N., Sierpowska, J., François, C., Càmara, E., van Vugt, F. T., Mohammadi, B., Samii, A., Münte,

- T. F., Rodríguez-Fornells, A., and Altenmüller, E. (2016). Structural neuroplasticity in expert pianists depends on the age of musical training onset. *NeuroImage*, 126(Supplement C):106 – 119.
- von Neumann, J. (1955). *Mathematical Foundations of Quantum Mechanics*. Princeton University Press.
- Woolhouse, M. (2009). Modelling tonal attraction between adjacent musical elements. *Journal of New Music Research*, 38(4):357 – 379.
- Woolhouse, M. (2012). Wagner in the round: using interval cycles to model chromatic harmony. In Cambouropoulos, E., Tsougras, C., Mavromatis, P., and Pantiadis, K., editors, *Proceedings of the 12th International Conference on Music Perception and Cognition and the 8th Triennial Conference of the European Society for the Cognitive Sciences of Music*, pages 1142 – 1145.
- Woolhouse, M. and Cross, I. (2010). Using interval cycles to model Krumhansl’s tonal hierarchies. *Music Theory Spectrum*, 32(1):60 – 78.
- Wright, J. J., Alexander, D. M., and Bourke, P. D. (2006). Contribution of lateral interactions in V1 to organization of response properties. *Vision Research*, 46:2703 – 2720.